Supporting online information for

Spectroscopic characterization of a Ru(III)-OCl intermediate: A structural mimic for haloperoxidase enzyme

Rakesh Kumar, Ayushi Awasthi, Sikha Gupta, Raju Eerlapally and Apparao Draksharapu*

Department of Chemistry, Indian Institute of Technology Kanpur, Kanpur–208016 (India)

Material and Methods

Synthesis of N^1-benzyl-N^1,N^2,N^2-tris(pyridin-2-ylmethyl)ethane-1,2-diamine (BnTPEN): Synthesis of BnTPEN ligand was carried out by modified literature procedure.[1] Picolylchloride hydrochloride salt (1.64 g, 10 mmol) was dissolved in 15 mL H_2O followed by the addition of N^1-benzylethane-1,2-diamine (500 mg, 3.33 mmol) in a 50 mL round-bottom flask equipped with a stir bar. Aqueous NaOH solution (800 mg in 10 mL) was added dropwise over a period of an hour and the reaction was stirred at room temperature for 7 days. After 7 days the reaction mixture was extracted in methylene chloride (3 x 25 mL). The combined organic phases were dried over Na_2SO_4 followed by the solvent evaporation under reduced pressure. Recrystallization from hot hexane yielded block like crystals of BnTPEN in 4 to 6 h. Yield: 940 mg, 66.7%. Characterization: ^{1}H NMR ($CDCl_3$, 400 MHz): δ (ppm) 8.50-8.47 (m, 3H), 7.59-7.56 (m, 3H), 7.45 (dd, 3H, J = 19.25 Hz, 8 Hz), 7.30-7.27 (m, 3H), 7.25-7.20 (m, 2H), 7.13-7.10 (m, 3H), 3.78 (s, 4H), 3.73 (s, 2H), 3.59 (s, 2H), 2.77-2.74 (m, 2H), 2.72-2.69 (m, 2H). ^{13}C NMR ($CDCl_3$, 100 MHz): δ (ppm) 160.27, 159.84, 149.03, 148.87, 139.31, 136.44, 128.90, 128.29, 126.99, 122.88, 121.96, 121.90, 60.88, 60.68, 59.12, 52.35, 52.02.

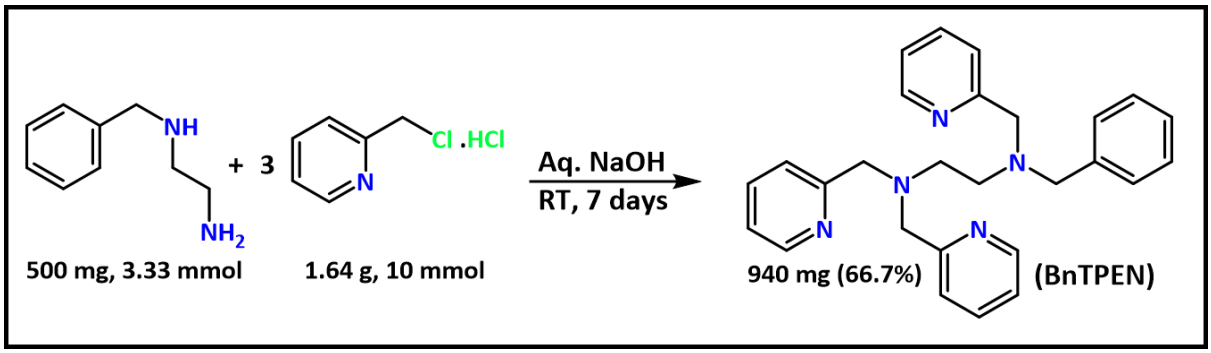

Scheme S1: Synthetic procedure for BnTPEN.

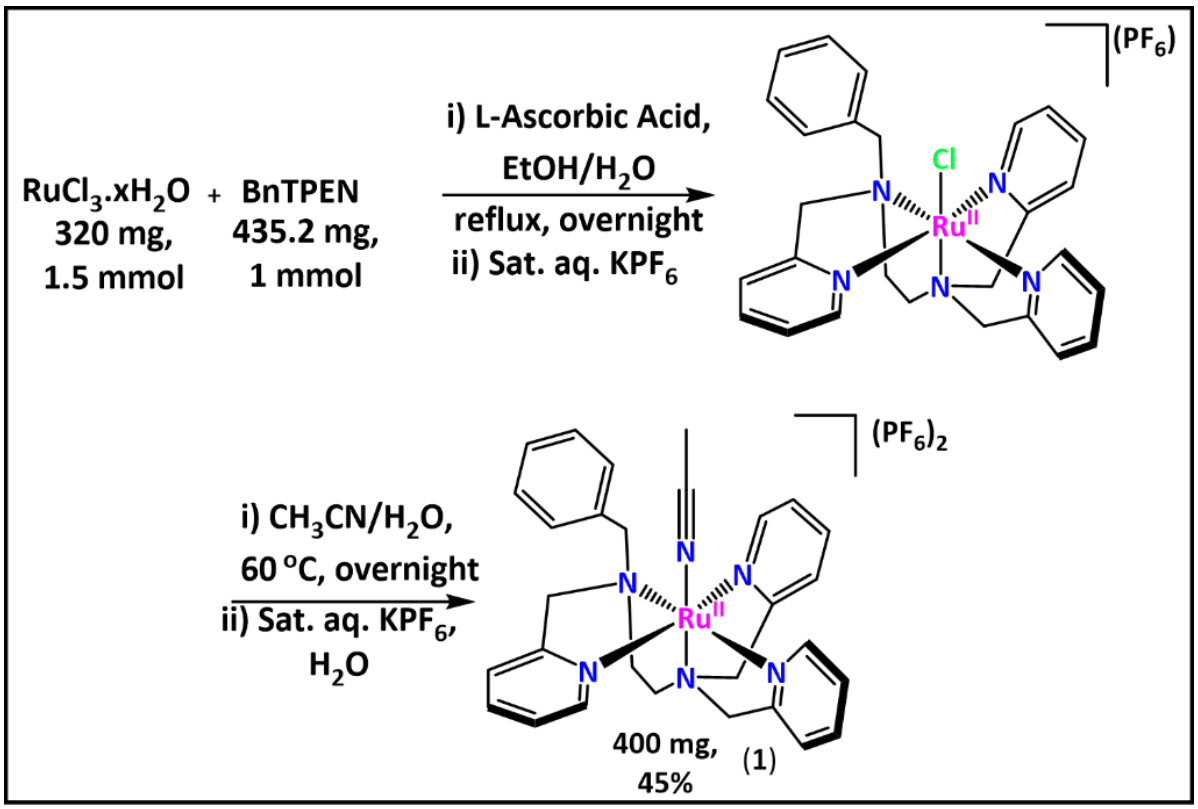

Scheme S2: Synthetic procedure for $[Ru^{II}(BnTPEN)(NCCH_3)](PF_6)_2$ (**1**).

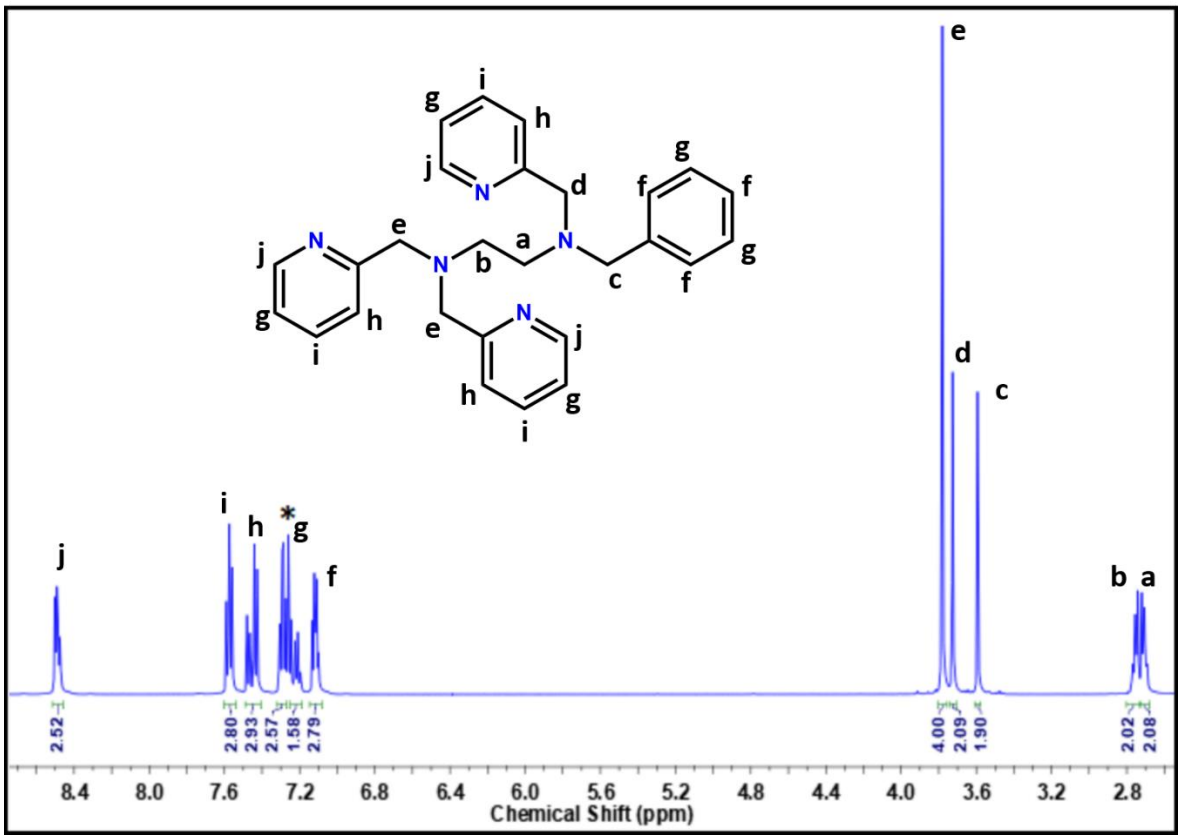

Figure S1: ^1H NMR spectrum of BnTPEN in $CDCl_3$ at 400 MHz. (* peak for solvent)

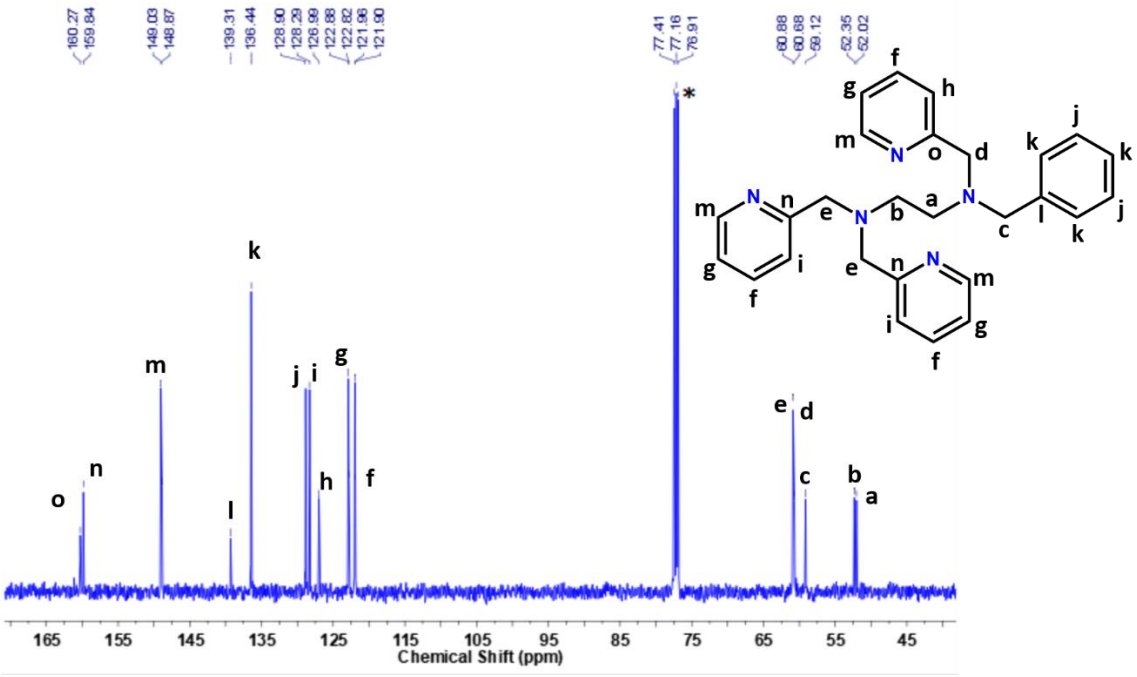

Figure S2: $^{13}C\{1H\}$ NMR spectrum of BnTPEN in $CDCl_3$ at 100 MHz. (* peak for solvent)

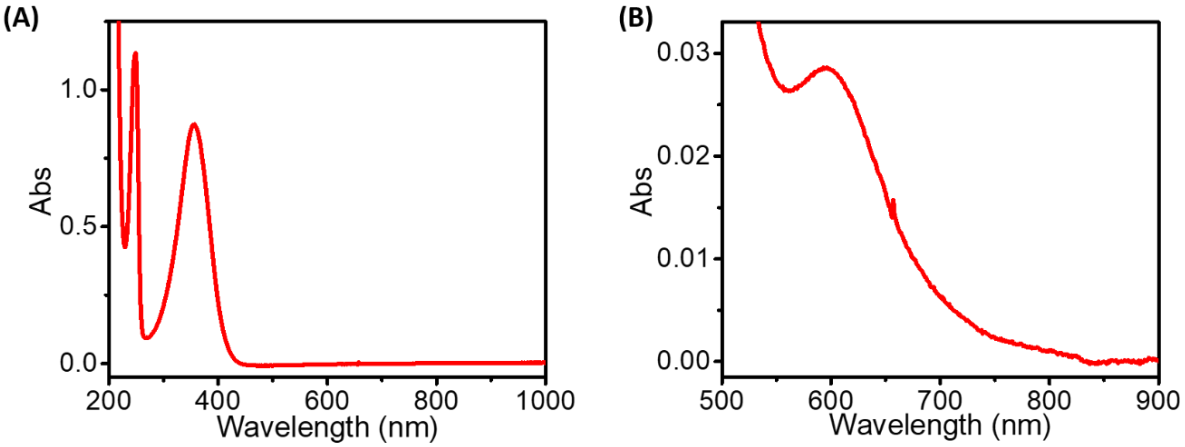

Figure S3: UV/Vis absorption spectra (A) 0.06 mM and (B) 4 mM of $[Ru^{II}(BnTPEN)(NCCH_3)](PF_6)_2$ (**1**) in CH_3CN at room temperature. d-d transition at 595 nm is visible at higher concentrations.

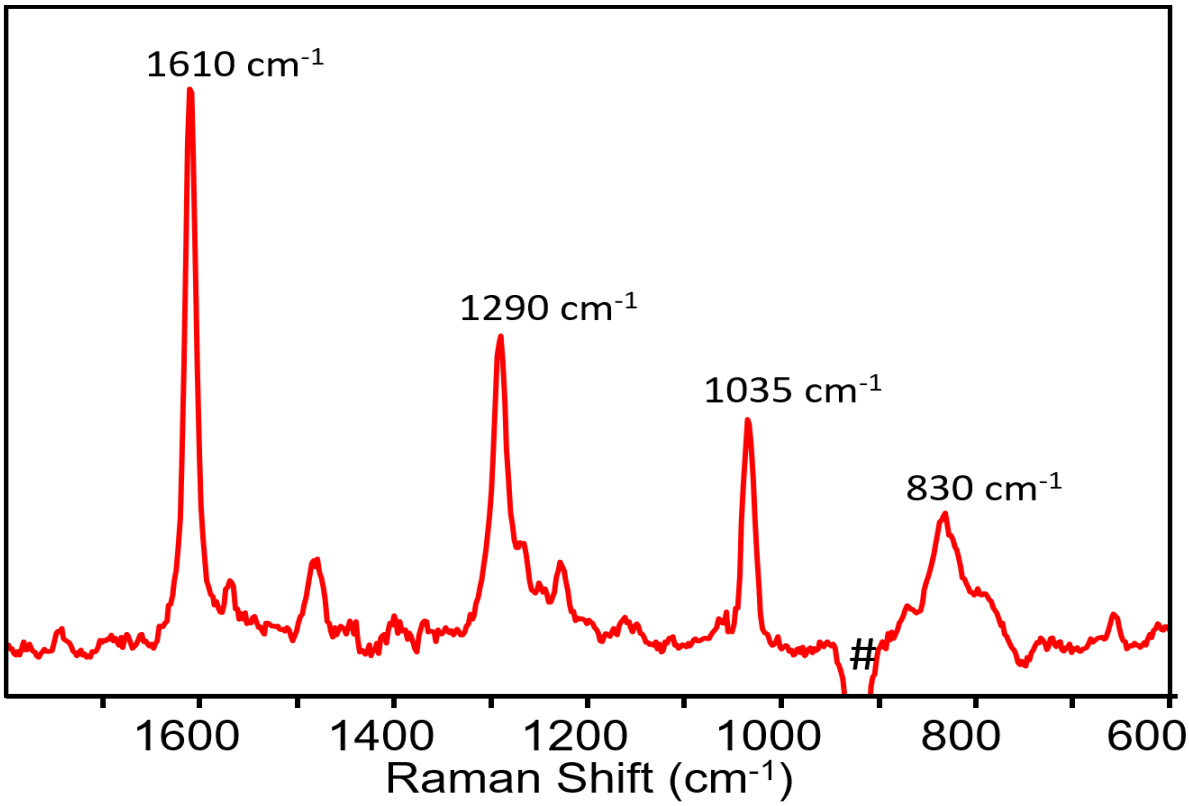

Figure S4: Solvent subtracted resonance Raman spectrum of **1** in acetonitrile at λ_{exc} = 405 nm. #Indicate imperfect solvent subtraction.

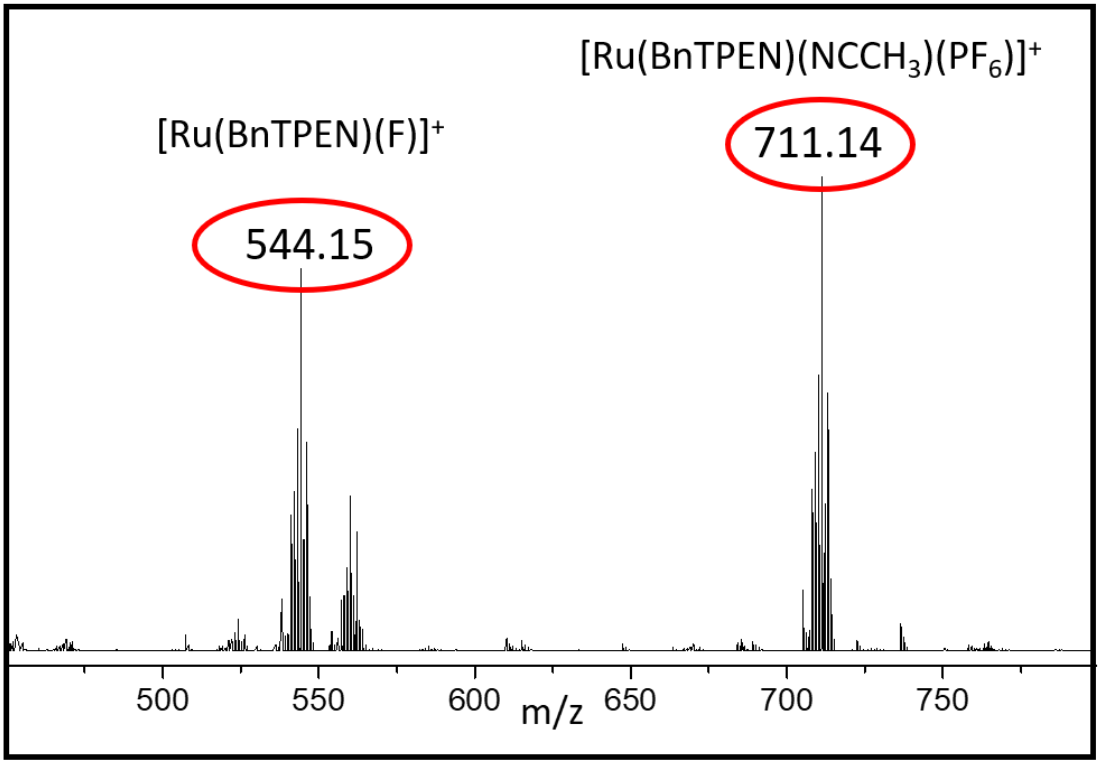

Figure S5: Positive mode ESI-mass spectrum of **1** in CH_3CN.

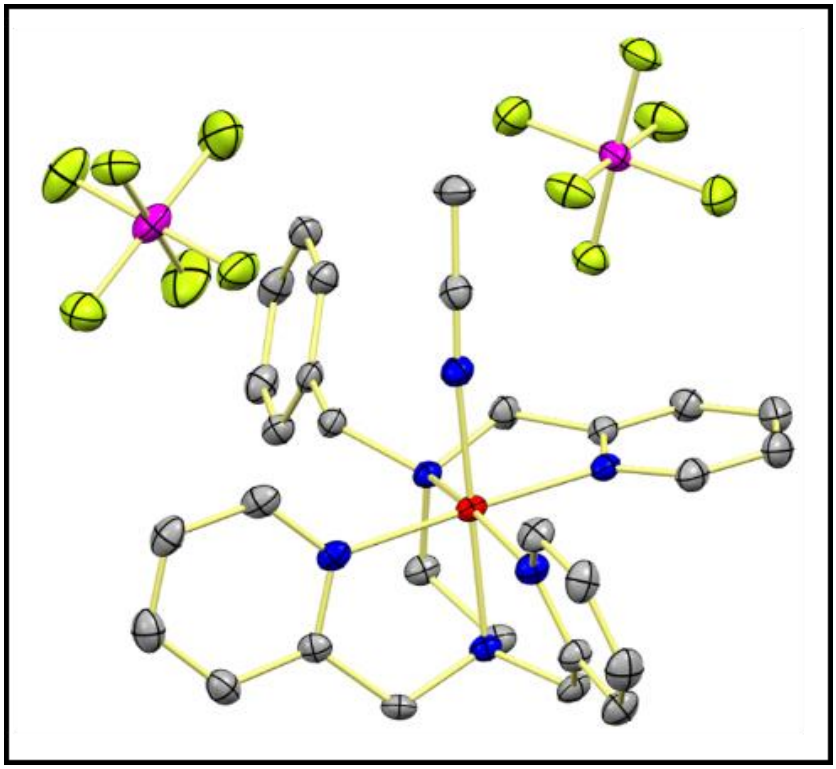

Figure S6: X-ray crystal structure of $[Ru^{II}(BnTPEN)(NCCH_3)](PF_6)_2$ (**1**). Hydrogen atoms were omitted for clarity.

Table S1: Crystal data and structure refinement of **1**.

Empirical formula	$C_{29}H_{32}F_{12}N_6P_2Ru$
Formula weight	855.61
Temperature/K	100
Crystal system	orthorhombic
Space group	Pbca
a/Å	17.8918(13)
b/Å	18.6494(14)
c/Å	19.6329(15)
α/°	90
β/°	90
γ/°	90
Volume/Å^3	6550.9(8)
Z	8
ρ_{calc}g/cm^3	1.735
μ/mm^{-1}	0.678
F(000)	3440.0

Crystal size/mm^3	0.2 × 0.18 × 0.16
Radiation	MoKα (λ = 0.71073)
2Θ range for data collection/°	5.346 to 56.608
Index ranges	-23 ≤ h ≤ 23, -24 ≤ k ≤ 24, -26 ≤ l ≤ 26
Reflections collected	93737
Independent reflections	8125 [R_{int} = 0.0807, R_{sigma} = 0.0380]
Data/restraints/parameters	8125/0/452
Goodness-of-fit on F^2	1.075
Final R indexes [I>=2σ (I)]	R_1 = 0.0451, wR_2 = 0.0822
Final R indexes [all data]	R_1 = 0.0689, wR_2 = 0.0937
Largest diff. peak/hole / e $Å^{-3}$	0.82/-0.62

Table S2: Selected Bond lengths (Å) of **1** and bond distance comparison with $[Ru^{II}(TPA)(NCCH_3)_2](PF_6)_2$ and $[Ru^{II}(N4Py)(OH_2)](PF_6)_2$. [2, 3]

	1	**$[Ru^{II}(TPA)(NCCH_3)_2](PF_6)_2$[a]**	**$[Ru^{II}(N4Py)(OH_2)](PF_6)_2$[b]**
Atom	**Length/Å**	**Length/Å**	**Length/Å**
$Ru\text{-}N_{py}$	2.067(3) 2.060(3) 2.071(3)	2.062(4) 2.071(4) 2.056(4)	2.057(4) 2.052(4) 2.061(4) 2.060(5)
$Ru\text{-}N_{amine}$	2.069(3) 2.141(2)	2.053(4)	1.967(5)
$Ru\text{-}N_{MeCN}$	2.030(3)	2.031(5) 2.037(5)	
$Ru\text{-}O_{water}$			2.172(5)
$Ru\text{-}N_{Avg}$	2.073	2.051	2.039

[a] TPA: tris(2-pyridylmethyl)amine;

[b] N4Py: N,N-bis(2-pyridyl-methyl)-N-bis(2-pyridyl)methylamine)

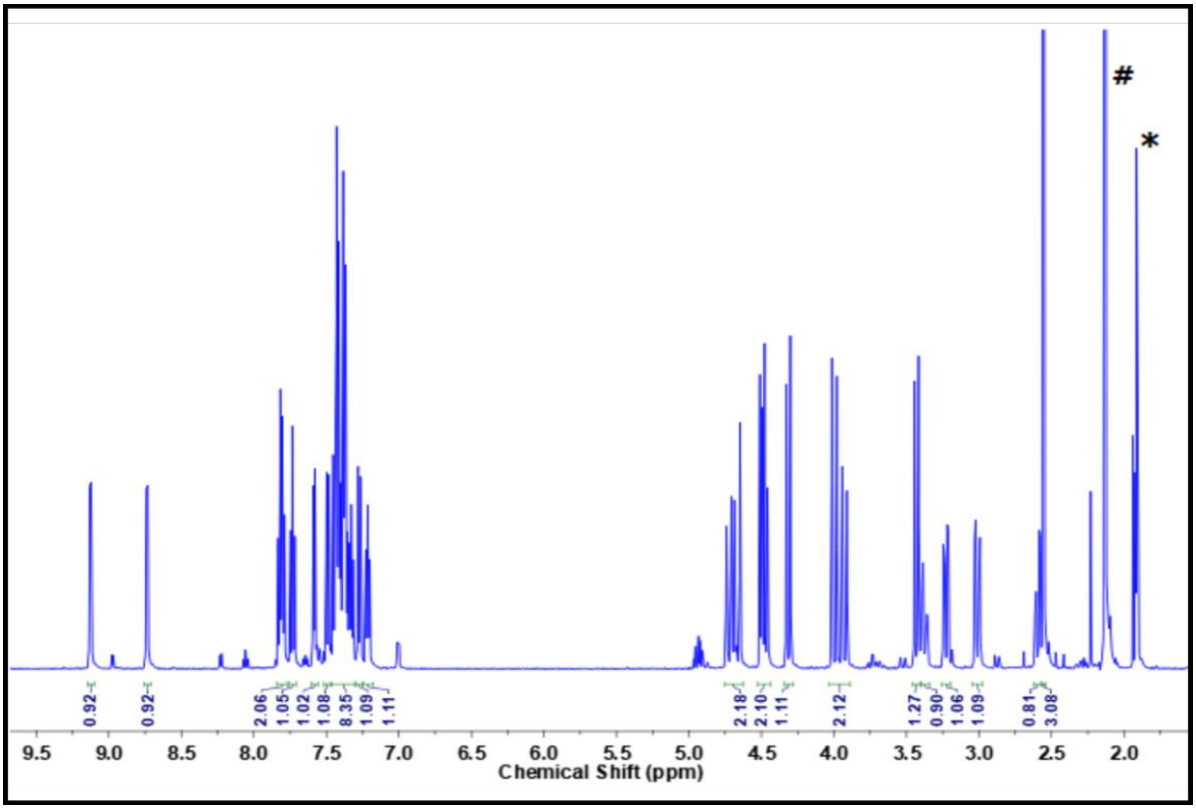

Figure S7: ^{1}H NMR spectrum of **1** in CD_3CN at 500 MHz. (*peak for solvent, $^{\#}$peak for H_2O)

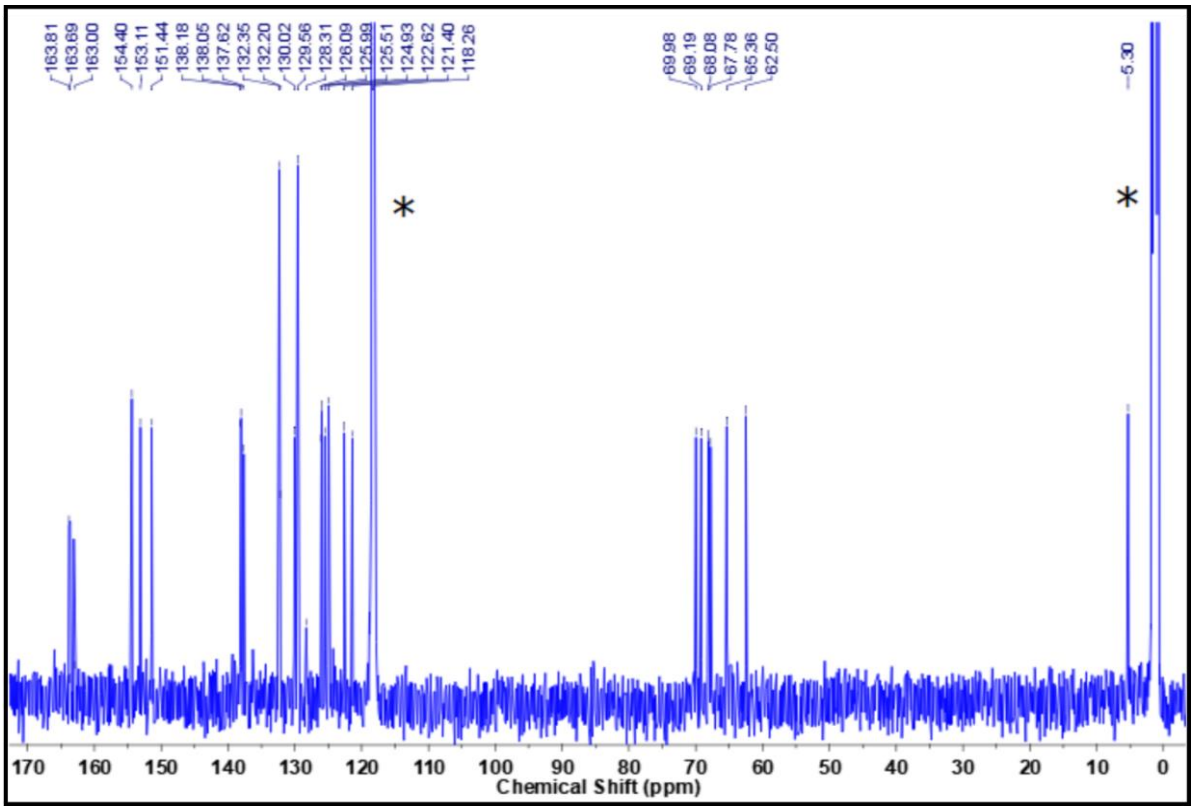

Figure S8: $^{13}C\{1H\}$ NMR spectrum of **1** in CD_3CN at 125 MHz. (*peak for solvent)

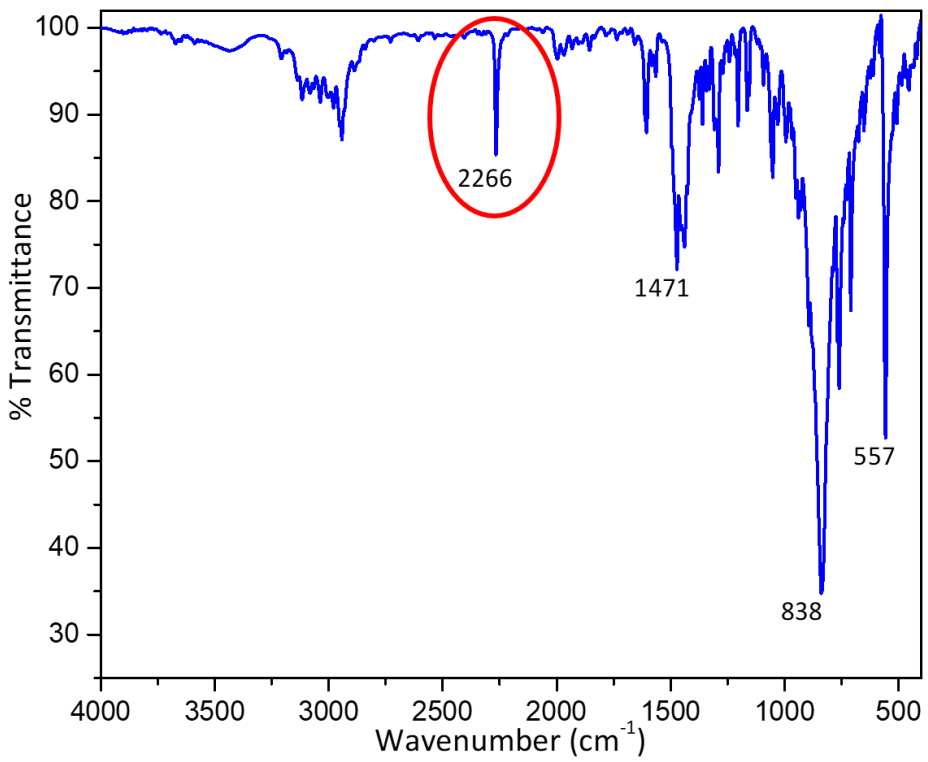

Figure S9: Solid-state FT-IR spectrum of **1** on KBr pellet. The band at 2266 cm^{-1} is originated from the bound acetonitrile molecule to **1**.

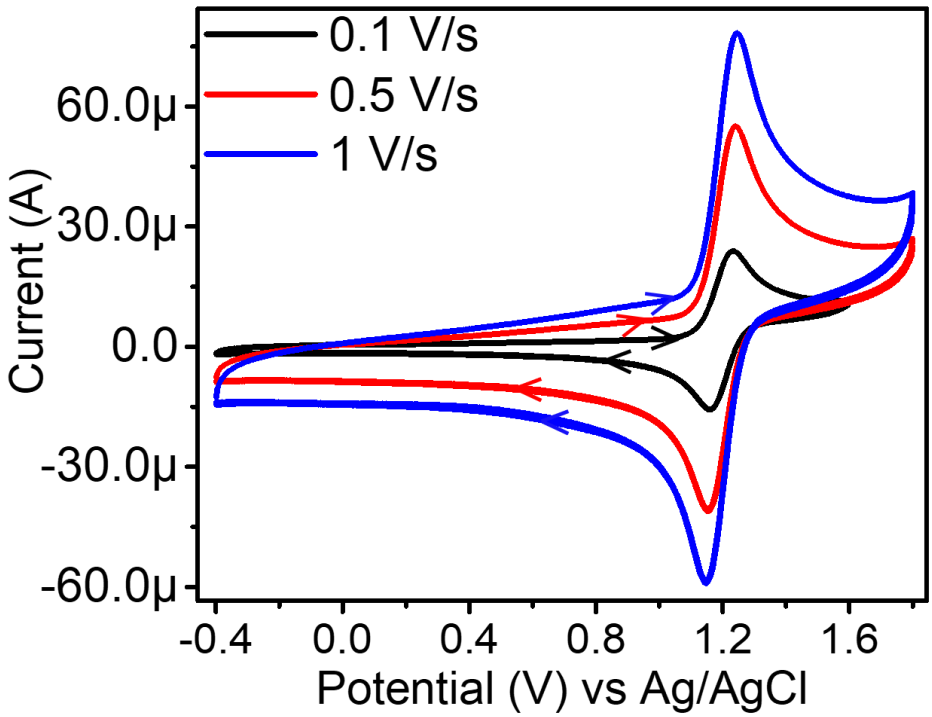

Figure S10: Scan rate (in V/s) dependent cyclic voltammograms of **1** in CH_3CN in the positive direction. Starting point of each scan started at open circuit potential (typically, between 0 to 0.3 V).

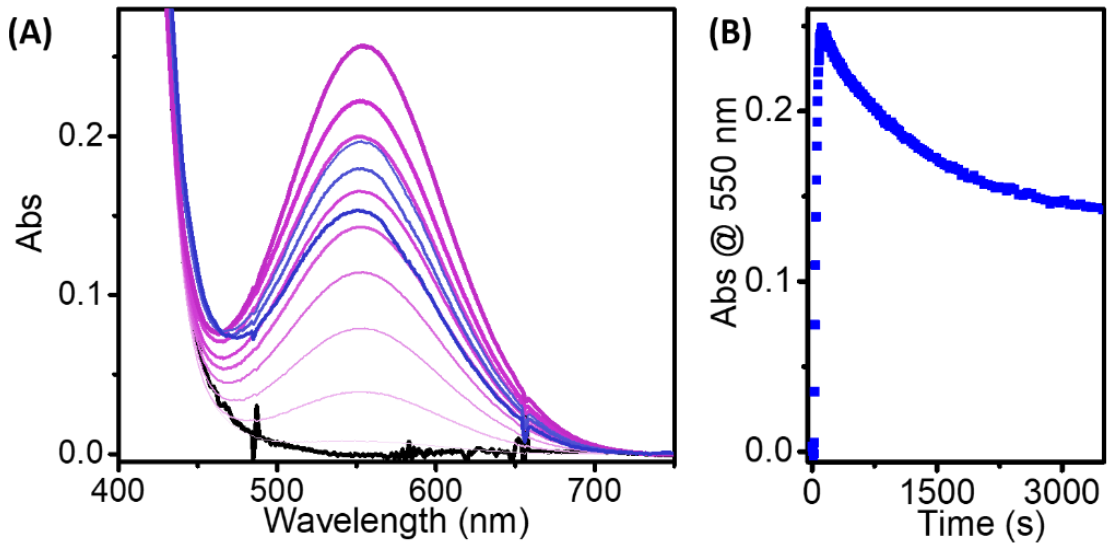

Figure S11: (A) Time-dependent UV/Vis absorption spectral changes upon the reaction of **1** (0.5 mM in CH_3CN) with 10 eq. $HClO_4$ and 10 eq. aqueous NaOCl at room temperature. (B) Corresponding changes in the absorption at 550 nm over time in seconds.

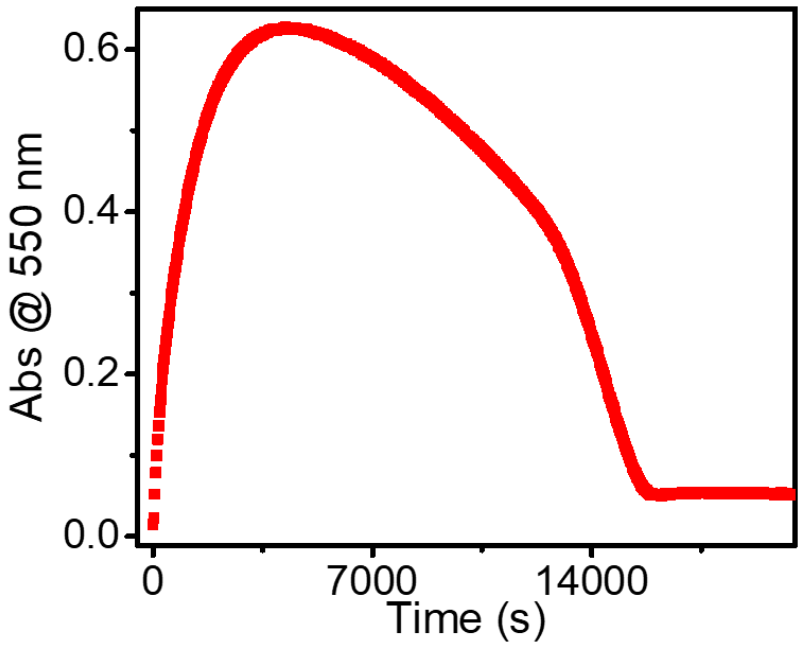

Figure S12: Time-dependent absorption changes at 550 nm of **2**, generated upon the reaction of **1** (0.5 mM) with 10 eq. $HClO_4$ and 10 eq. aqueous NaOCl in 3:1 CH_3CN:H_2O at RT. The intermediate **2** persisted for 4.5 h under the conditions employed.

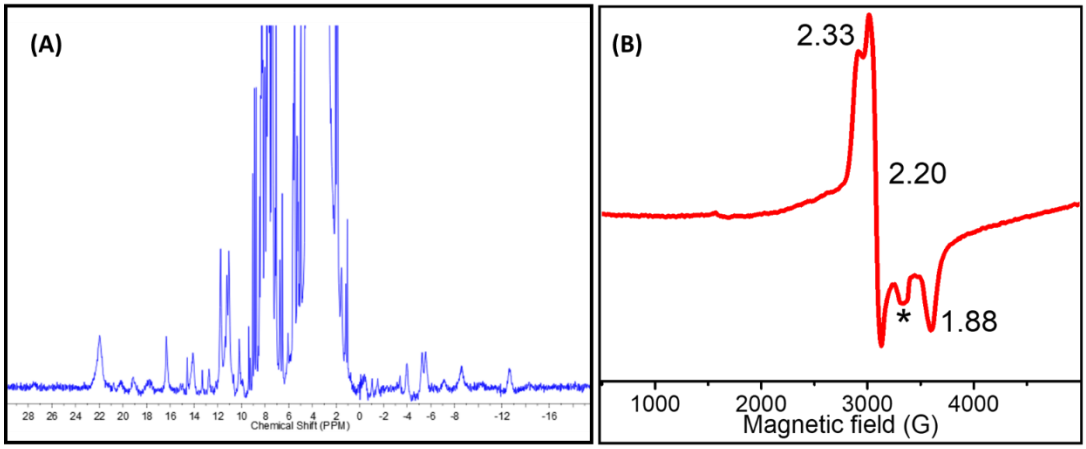

Figure S13: (A) ^{1}H NMR spectrum of **2** in (3:1) $CD_3CN:D_2O$ at 500 MHz. *Condition to generate **2**: 70 mM of **1** in 3:1 $CD_3CN:D_2O$ with 10 eq. $HClO_4$ and 10 eq. aqueous NaOCl.* (B) Full-scale X-band EPR spectrum of **2** generated by the reaction of 0.5 mM **1** with 10 eq. $HClO_4$ and 10 eq. aqueous NaOCl in 3:1 $CH_3CN:H_2O$ at 120 K. * Artifact from the cavity.

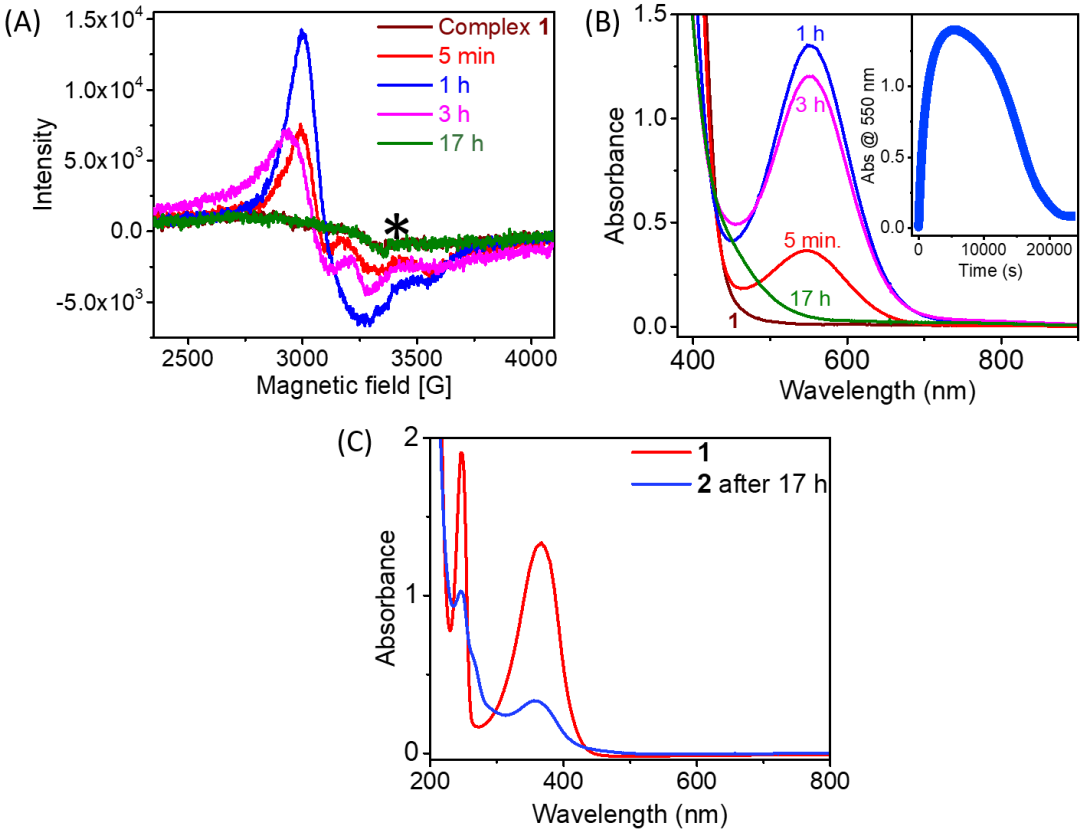

Figure S14: (A) Reaction progress for the formation and decay of **2** followed by X-band EPR spectroscopy obtained at 120 K. Modulation amplitude 1.98 G; Modulation frequency 100 KHz, and Attenuation 10 dB. *Artifact from the cavity. (B) The corresponding UV/Vis absorption spectra of the samples used to run the EPR data. Inset: Absorption changes followed at 550 nm of **2**. Conditions: 1 mM **1** in 3:1 $CH_3CN:H_2O$, 10 eq. $HClO_4$, and 10 eq. aqueous NaOCl. (C) UV/Vis absorption spectral comparison of the decayed sample (17 h) of **2** and **1** (in 1 mm path length cuvette).

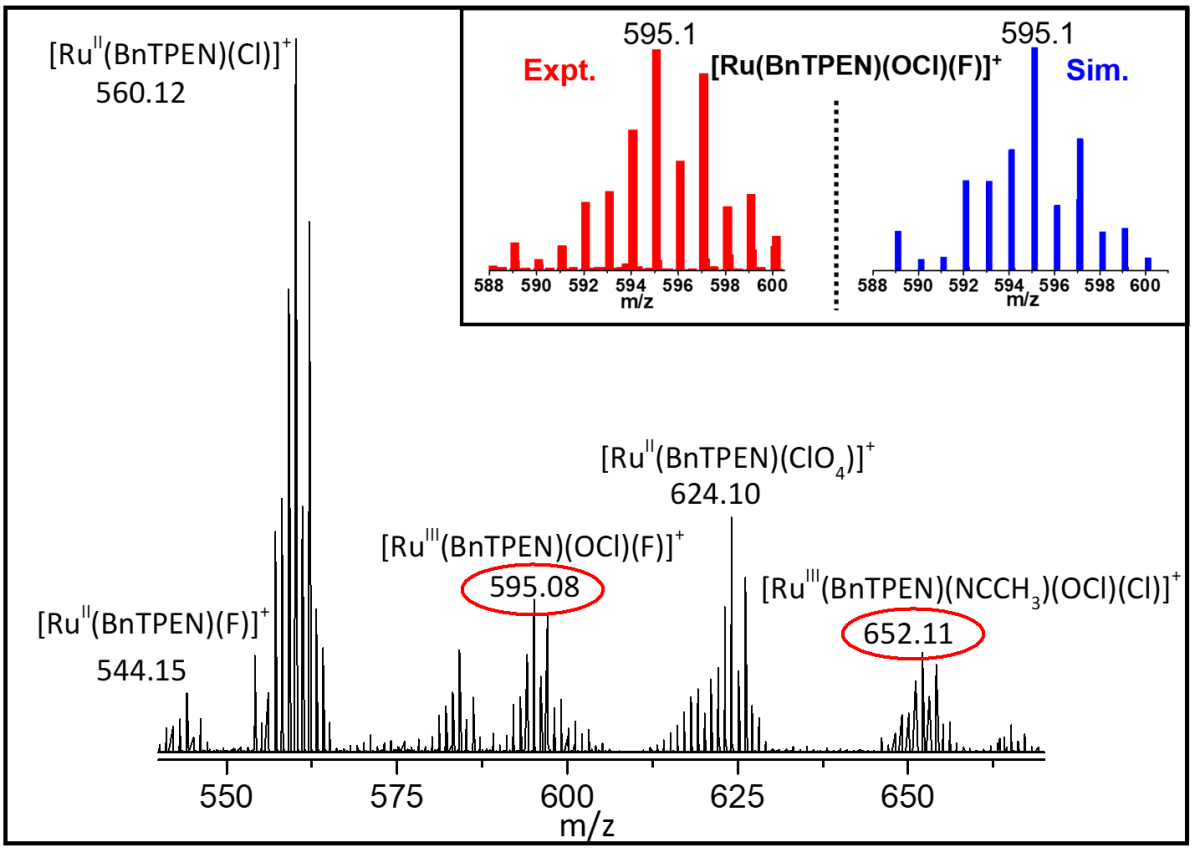

Figure S15: ESI-mass spectrum of **2**, generated upon the reaction of **1** with 10 eq. $HClO_4$ and 10 eq. aqueous NaOCl in 3:1 CH_3CN:H_2O at room temperature. Inset: ESI-mass spectrum experimental (left) and simulated (right) of **2**, formulated as $[Ru(BnTPEN)(OCl)(F)]^+$ (m/z: 595.1).

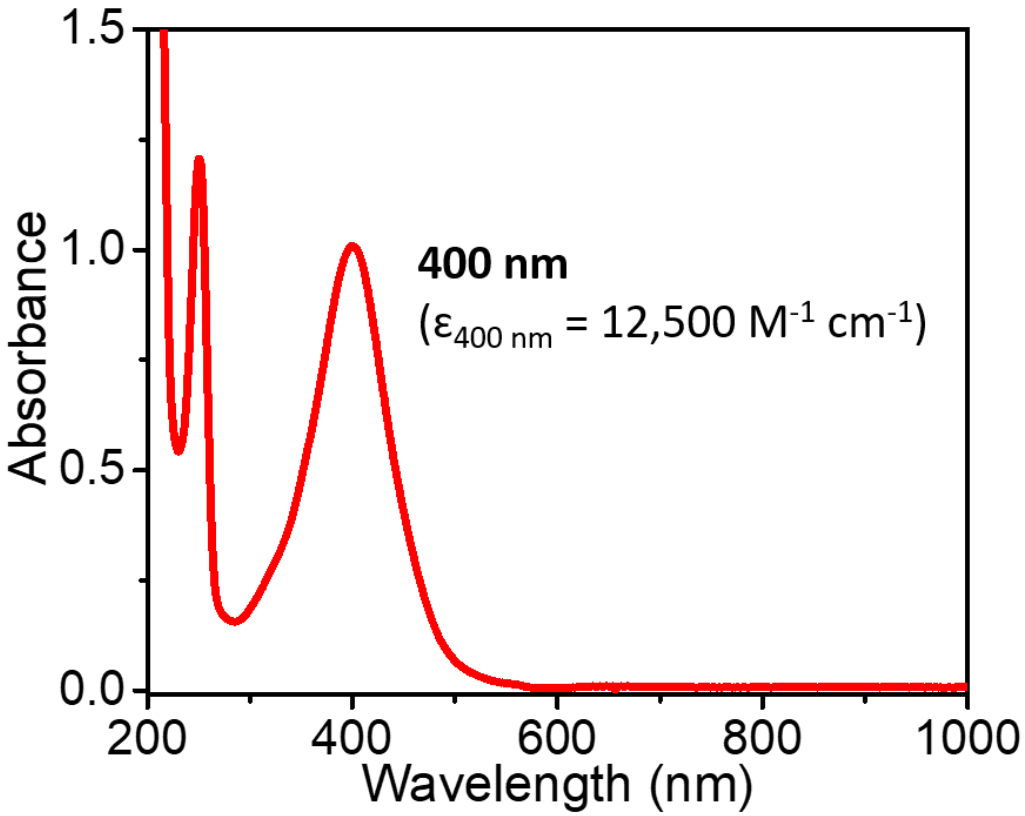

Figure S16: UV/Vis absorption spectrum of 0.08 mM [Ru^{II}(BnTPEN)(Cl)](Cl) (**3**) in CH_3CN at room temperature.

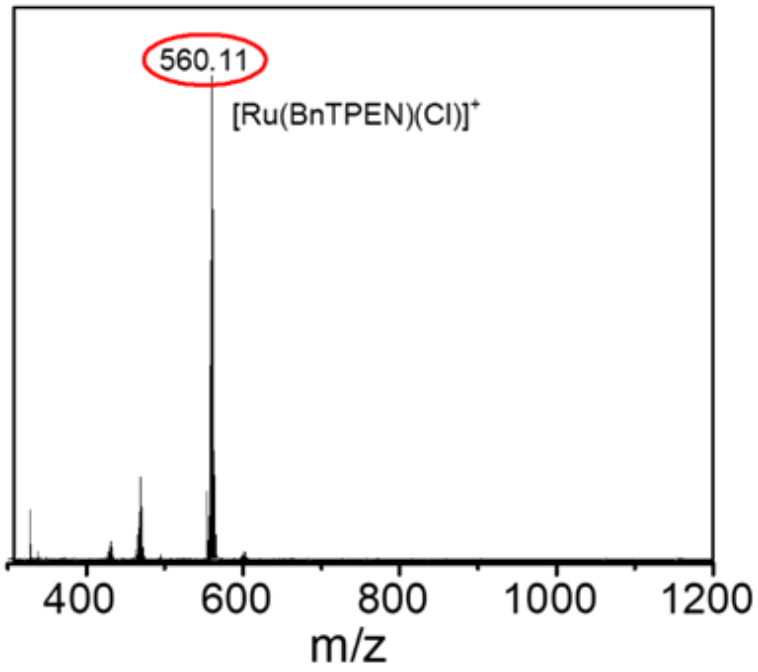

Figure S17: Positive mode ESI-mass spectrum of **3** in CH_3CN.

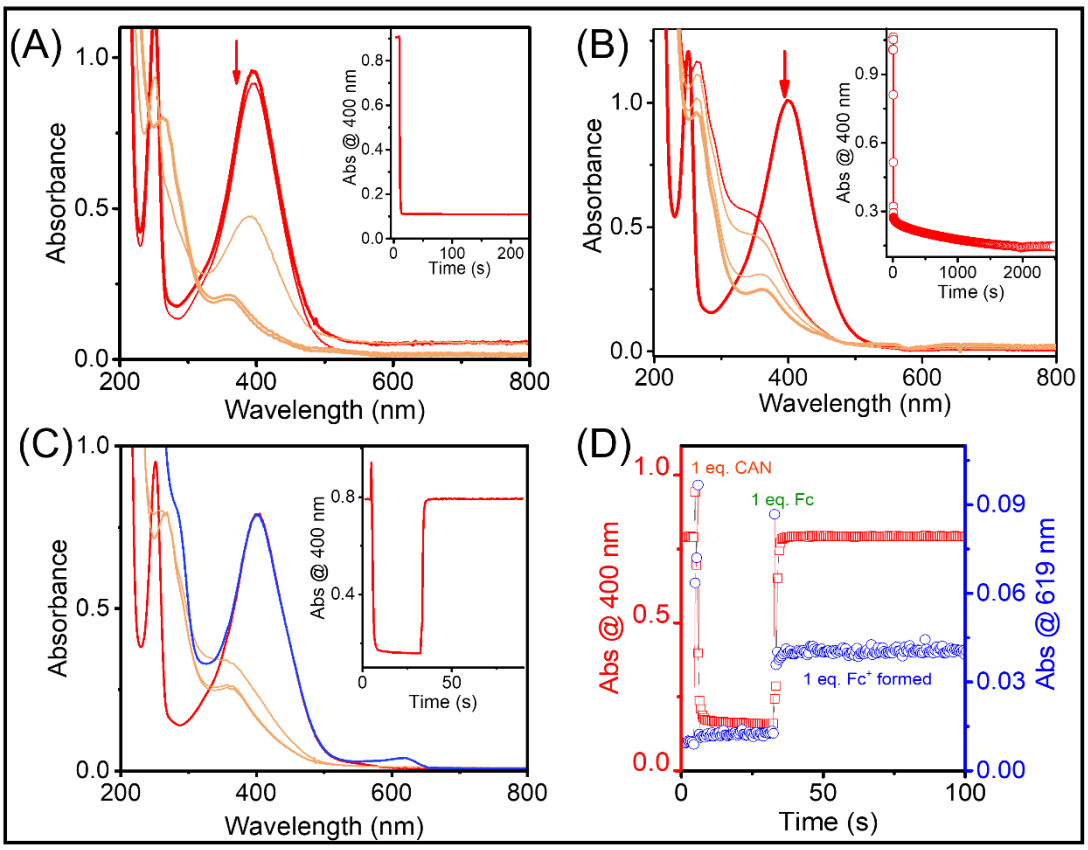

Figure S18: Time-dependent UV/Vis absorption spectral changes observed(A) upon the reaction of [Ru^{II}(BnTPEN)(Cl)](Cl) (0.08 mM in 3:1 CH_3CN:H_2O) with 10 eq. $HClO_4$ and 10 eq. aqueous NaOCl at room temperature. Inset: the corresponding changes in the absorption at 400 nm over time in seconds (B) upon the reaction of [Ru^{II}(BnTPEN)(Cl)](Cl) (0.08 mM in CH_3CN) with 1 eq. ammonium ceric nitrate at room temperature. Inset: the corresponding changes in the absorption at 400 nm over time in seconds. (C) Time-dependent UV/Vis absorption spectral changes upon the reaction of [Ru^{II}(BnTPEN)(Cl)](Cl) (0.08 mM in CH_3CN) with 1 eq. ammonium ceric nitrate (CAN) followed by the addition of 1 eq. ferrocene (Fc) at room temperature. Inset: the corresponding changes in the absorption at 400 nm over time in seconds. (D) Corresponding changes in the absorption at 400 nm for **3** and 619 nm for ferrocenium over time in seconds.

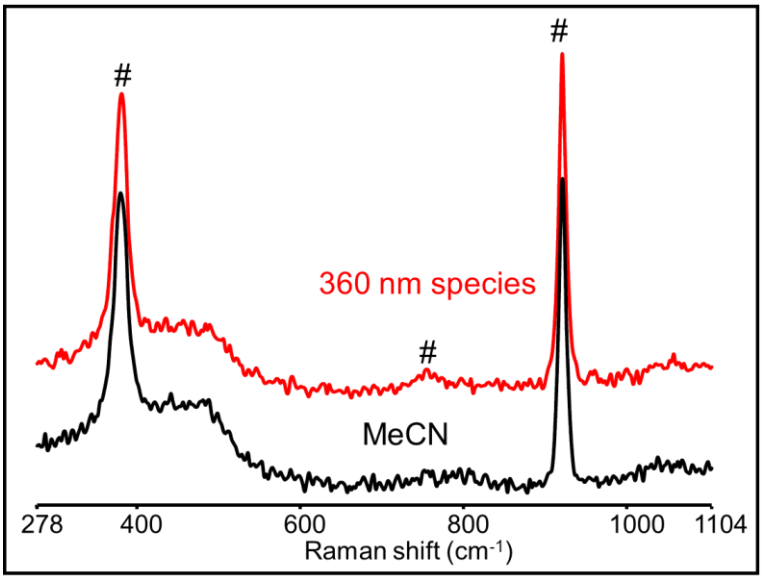

Figure S19: Raman spectrum of 360 nm species at λ_{exc} 532 nm generated by the reaction of [Ru(BnTPEN)(Cl)]Cl (1 mM) with 1 eq. CAN in acetonitrile at room temperature (Red); Raman spectrum of the solvent acetonitrile (Black). # Indicates solvent peaks.

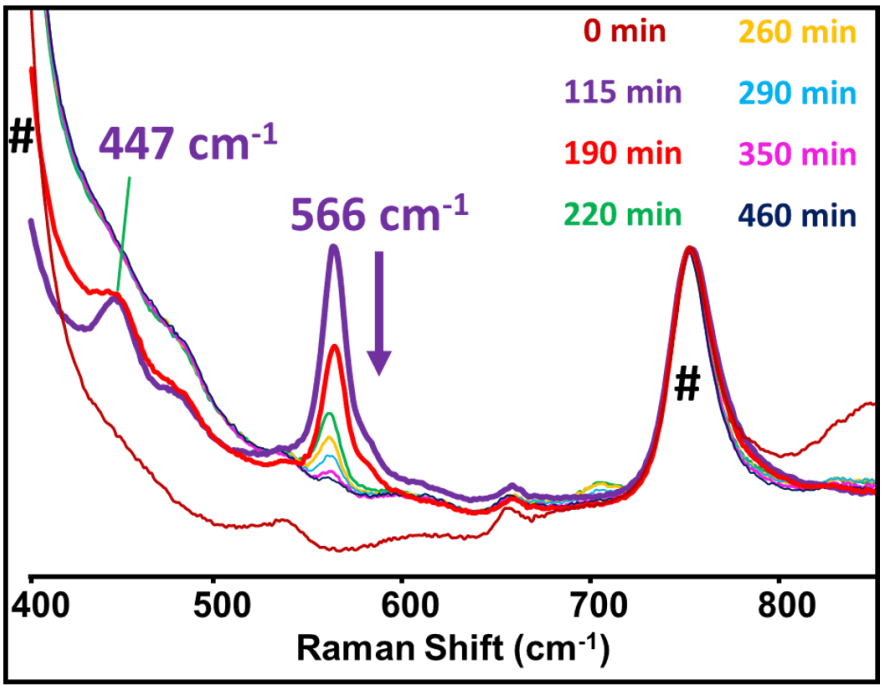

Figure S20: Time dependent resonance Raman spectra (at λ_{exc} 532 nm) of **2** in 3:1 $CH_3CN:H_2O$ generated by the addition of 10 eq. $HClO_4$ and 10 eq. aqueous NaOCl to **1** at room temperature. # Indicates solvent peaks.

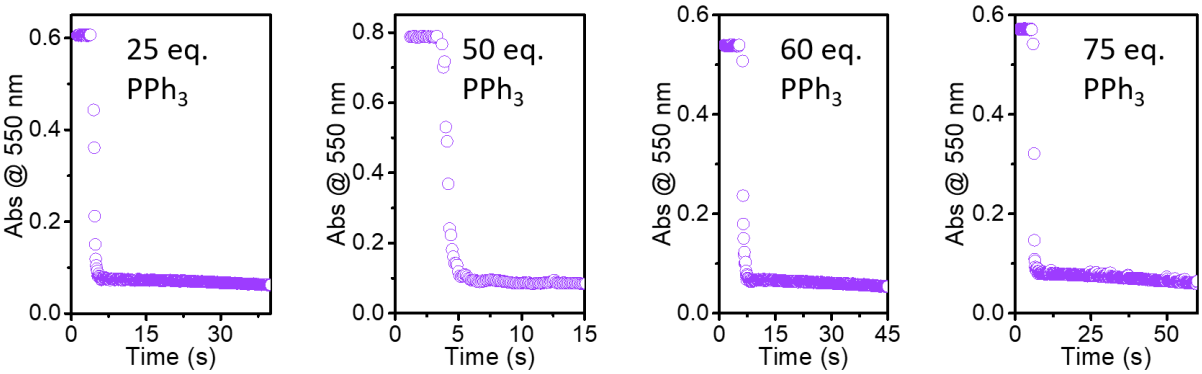

Figure S21: Decay of **2** followed at 550 nm in presence of various concentrations of PPh_3 in 3:1 CH_3CN: H_2O at 25 °C. *Conditions to generate **2**: 0.5 mM **1** in 3:1 CH_3CN:H_2O + 10 eq. $HClO_4$ and 10 eq. aqueous NaOCl*. Note: This reaction is too fast to reliably measure the rate under the conditions employed.

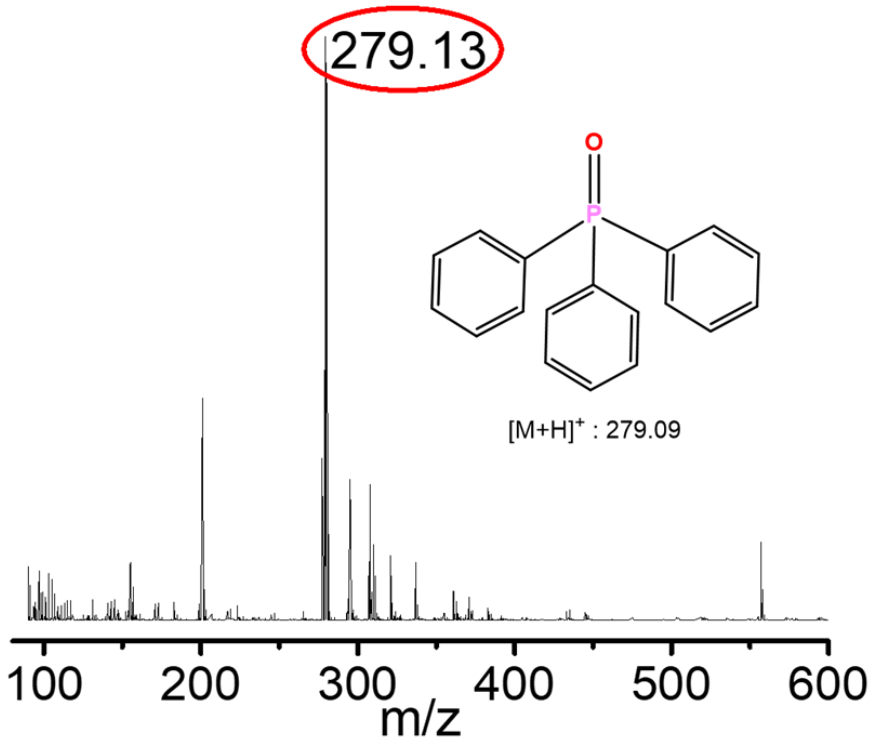

Figure S22: Product analysis of the reaction of **2** with 100 eq. PPh_3 by APCI-MS. Conditions to generate **2**: 2.0 mM **1** in 3:1 CH_3CN:H_2O + 10 eq. $HClO_4$ and 10 eq. aqueous NaOCl.

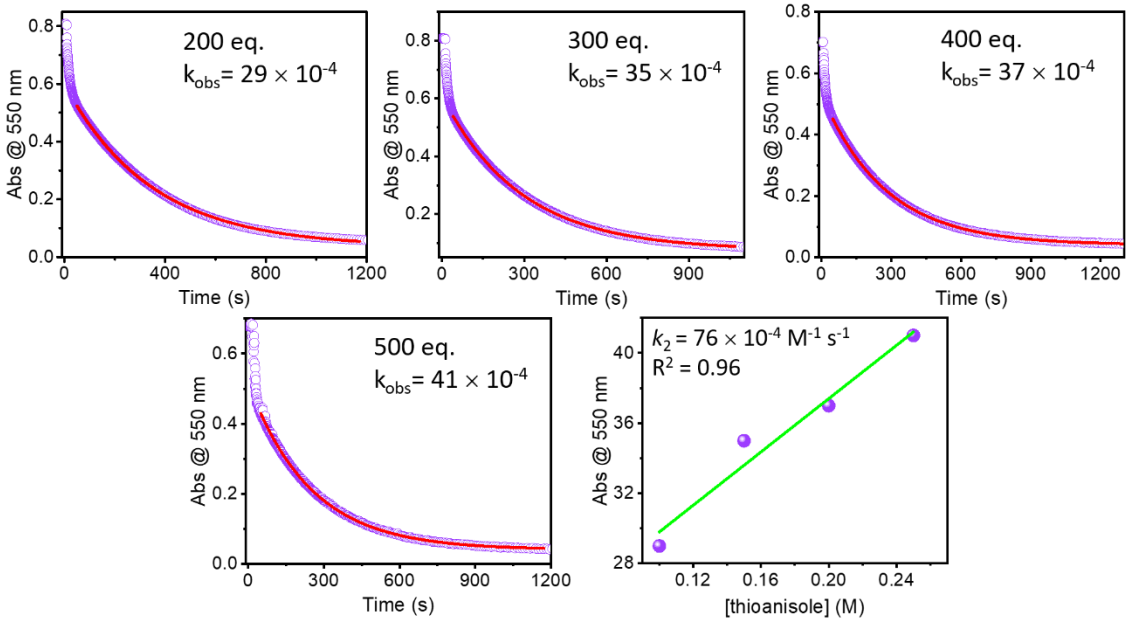

Figure S23: Decay of **2** followed at 550 nm in presence of various concentrations of thioanisole to give pseudo-first-order rate constants (k_{obs}) in 3:1 CH_3CN: H_2O at 25 °C. The plot of k_{obs} against the concentrations of thioanisole to obtain a second-order-rate constant (k_2 = 76 x 10^{-4} $M^{-1}s^{-1}$). *Conditions to generate **2**: 0.5 mM **1** in 3:1 CH_3CN:H_2O + 10 eq. $HClO_4$ and 10 eq. aqueous NaOCl*.

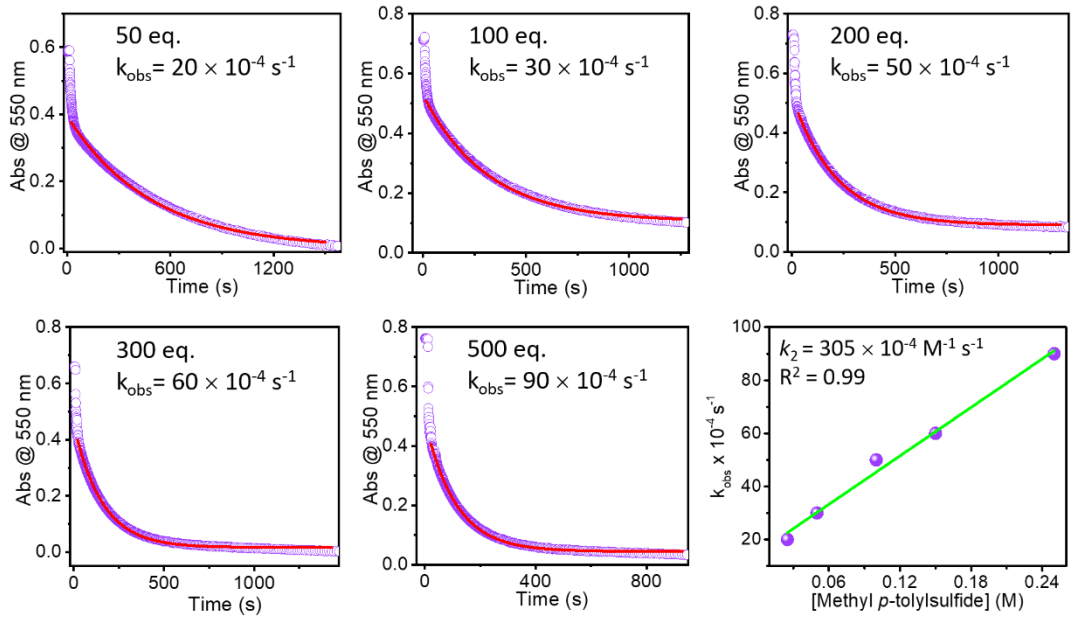

Figure S24: Decay of **2** followed at 550 nm in presence of various concentrations of methyl *p*-sulfide to give pseudo-first-order rate constants (k_{obs}) in 3:1 CH_3CN: H_2O at 25 °C. The plot of k_{obs} against the concentrations of methyl *p*-tolylsulfide to obtain a second-order-rate constant (k_2 = 305 x 10^{-4} $M^{-1}s^{-1}$). *Conditions to generate **2**: 0.5 mM **1** in 3:1 CH_3CN:H_2O + 10 eq. $HClO_4$ and 10 eq. aqueous NaOCl*.

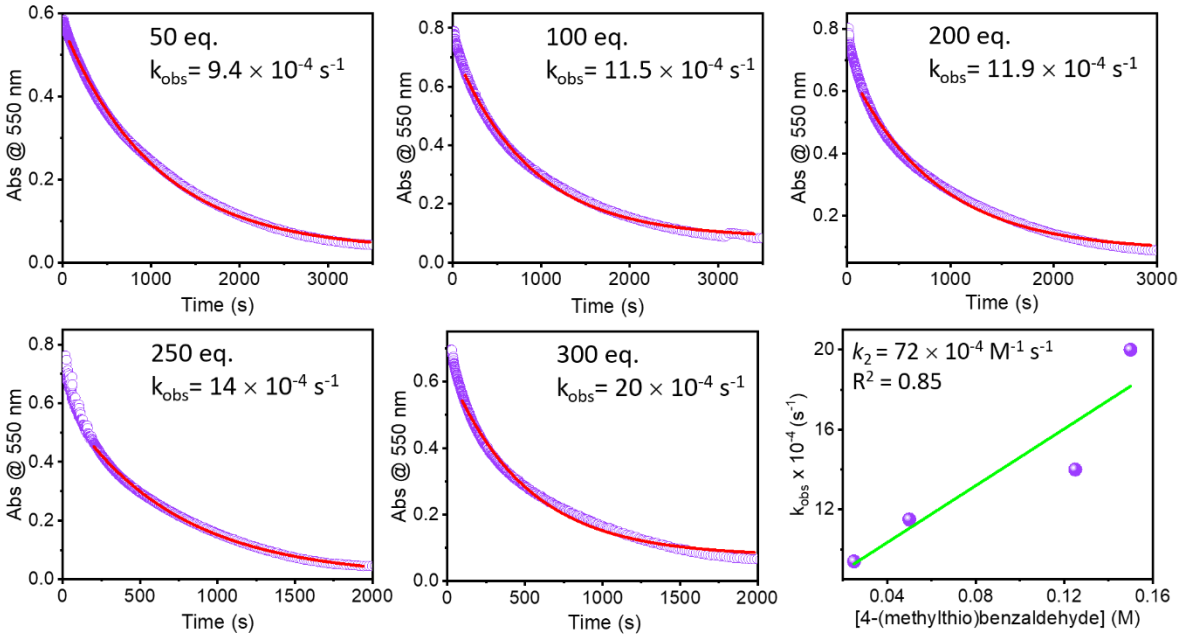

Figure S25: Decay of **2** followed at 550 nm in presence of various concentrations of 4-(methylthio)benzaldehyde to give pseudo-first-order rate constants (k_{obs}) in 3:1 CH_3CN: H_2O at 25 °C. The plot of k_{obs} against the concentrations of 4-(methylthio)benzaldehyde to obtain a second-order-rate constant (k_2 = 72 x 10^{-4} $M^{-1}s^{-1}$). *Conditions to generate **2**: 0.5 mM **1** in 3:1 CH_3CN:H_2O + 10 eq. $HClO_4$ and 10 eq. aqueous NaOCl*.

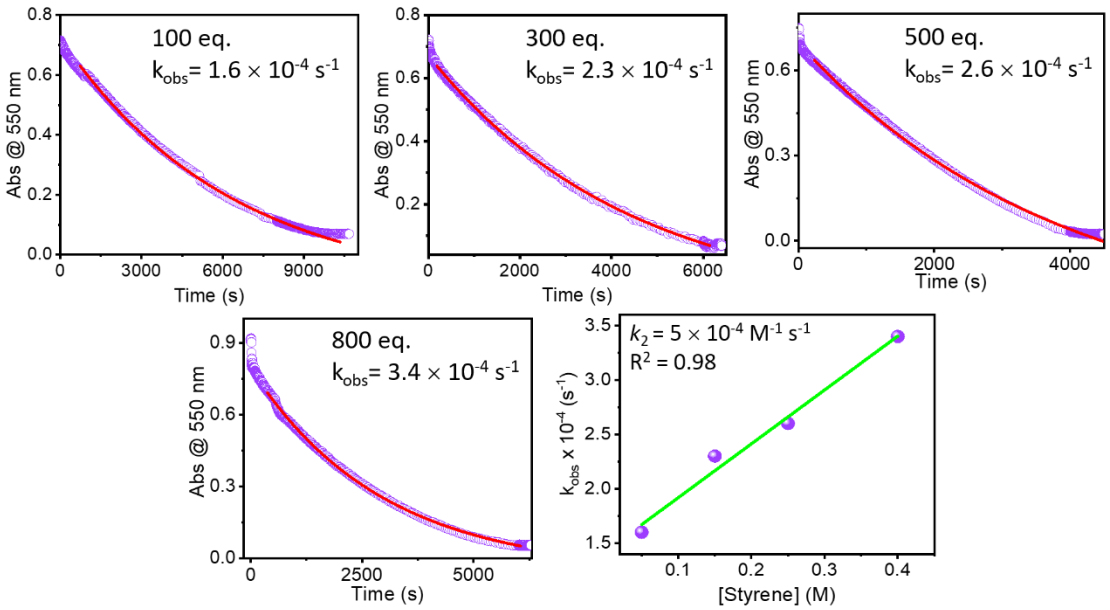

Figure S26: Decay of **2** followed at 550 nm in presence of various concentrations of styrene to give pseudo-first-order rate constants (k_{obs}) in 3:1 CH_3CN: H_2O at 25 °C. The plot of k_{obs} against the concentrations of styrene to obtain a second-order-rate constant (k_2 = 5 x 10^{-4} $M^{-1}s^{-1}$). *Conditions to generate **2**: 0.5 mM **1** in 3:1 CH_3CN:H_2O + 10 eq. $HClO_4$ and 10 eq. aqueous NaOCl*.

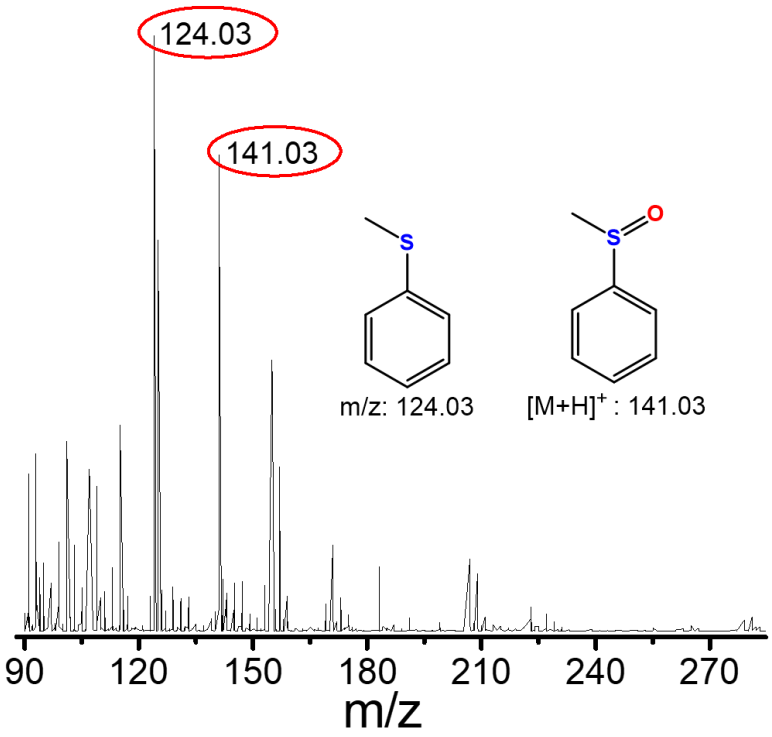

Figure S27: Product analysis of the reaction of **2** with 100 eq thioanisole by APCI-MS. Conditions to generate **2**: 2.0 mM **1** in 3:1 CH_3CN:H_2O + 10 eq. $HClO_4$ and 10 eq. aqueous NaOCl.

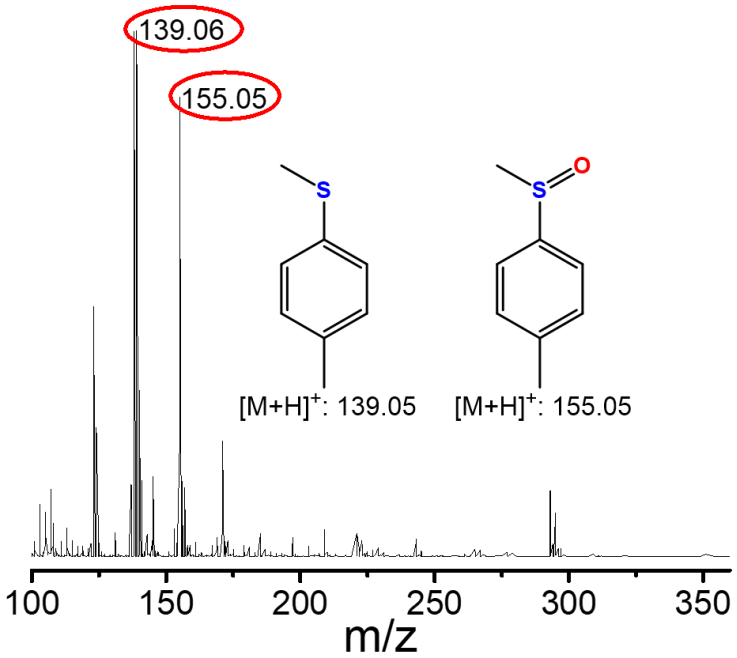

Figure S28: Product analysis of the reaction of **2** with 100 eq. methyl *p*-tolylsulfide by APCI-MS. Conditions to generate **2**: 2.0 mM **1** in 3:1 CH_3CN:H_2O + 10 eq. $HClO_4$ and 10 eq. aqueous NaOCl.

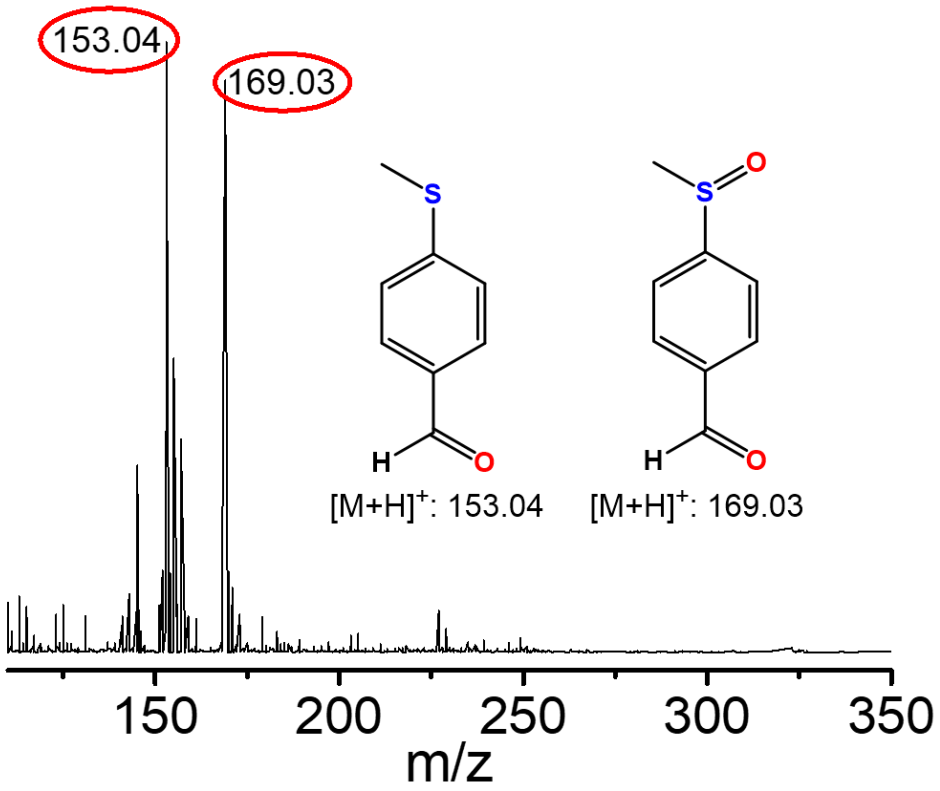

Figure S29: Product analysis of the reaction of **2** with 100 eq. 4-(methylthio)benzaldehyde by APCI-MS. Conditions to generate **2**: 2.0 mM **1** in 3:1 CH_3CN:H_2O + 10 eq. $HClO_4$ and 10 eq. aqueous NaOCl.

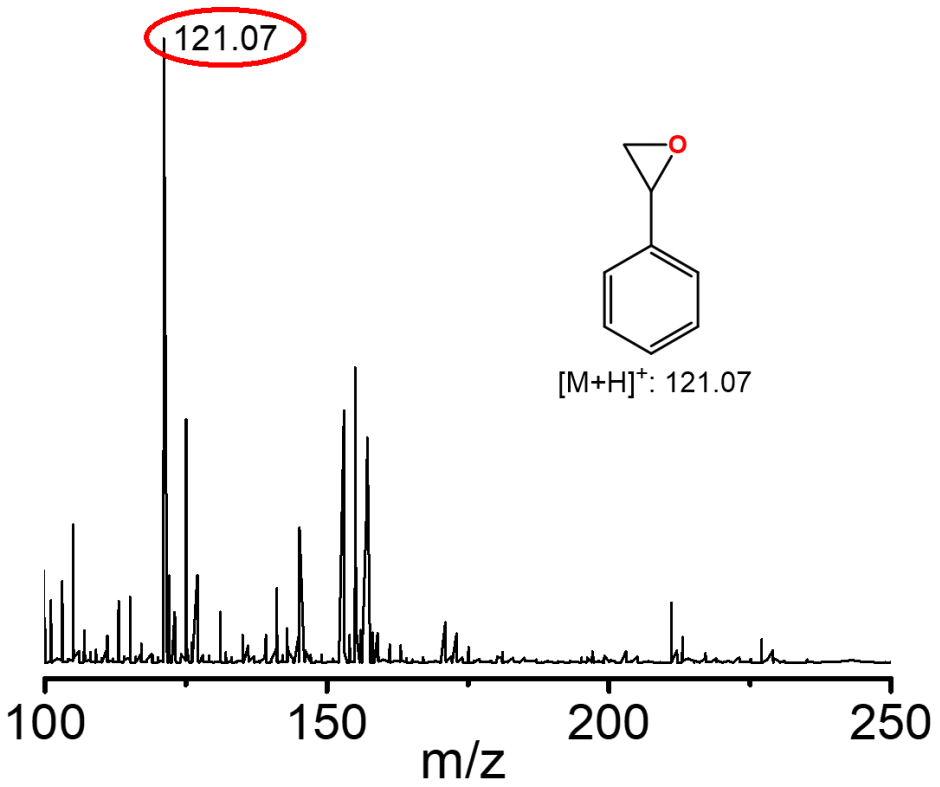

Figure S30: Product analysis of the reaction of **2** with 100 eq. styrene by APCI-MS. Conditions to generate **2**: 2.0 mM **1** in 3:1 CH_3CN:H_2O + 10 eq. $HClO_4$ and 10 eq. aqueous NaOCl.

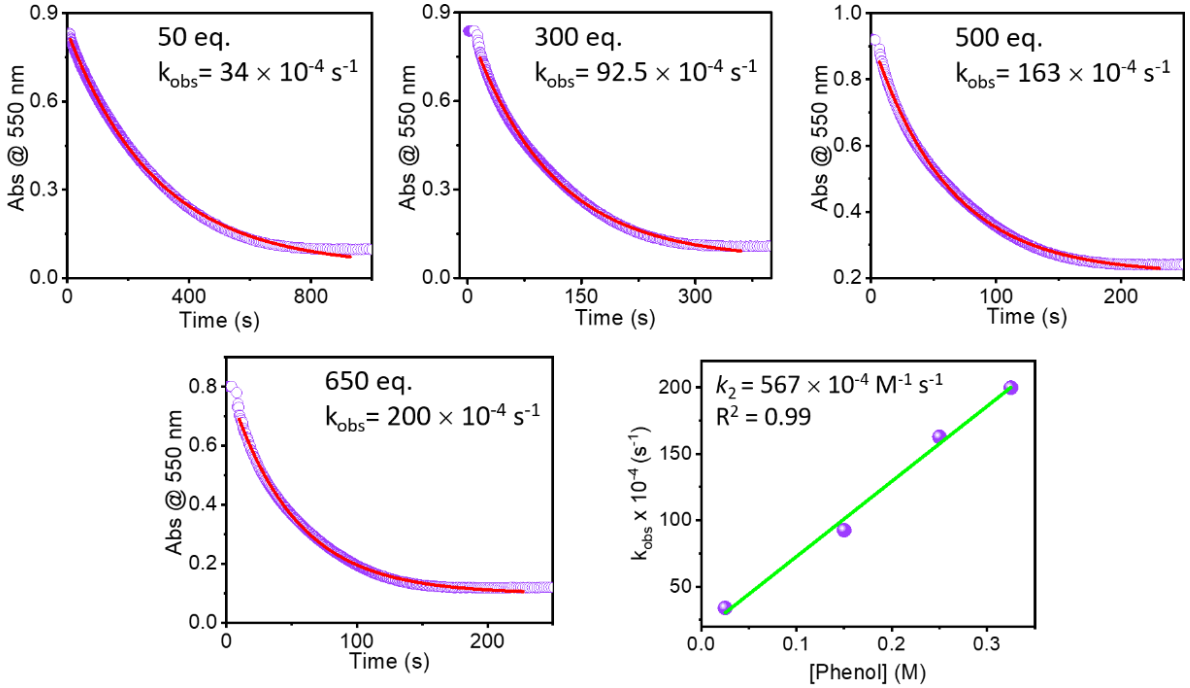

Figure S31: Decay of **2** followed at 550 nm in presence of various concentrations of phenol to give pseudo-first-order rate constants (k_{obs}) in 3:1 CH_3CN: H_2O at 25 °C. The plot of k_{obs} against the concentrations of phenol to obtain a second-order-rate constant (k_2 = 567 x 10^{-4} $M^{-1}s^{-1}$). *Conditions to generate **2**: 0.5 mM **1** in 3:1 CH_3CN:H_2O + 10 eq. $HClO_4$ and 10 eq. aqueous NaOCl*.

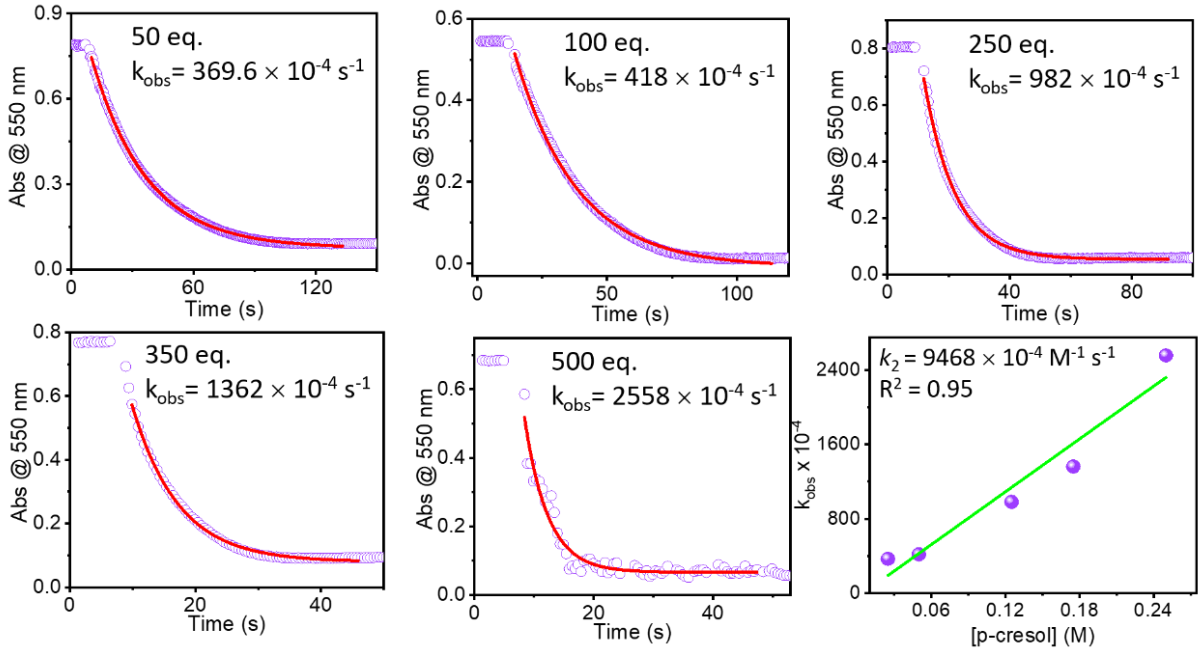

Figure S32: Decay of **2** followed at 550 nm in presence of various concentrations of *p*-cresol to give pseudo-first-order rate constants (k_{obs}) in 3:1 CH_3CN: H_2O at 25 °C. The plot of k_{obs} against the concentrations of *p*-cresol to obtain a second-order-rate constant (k_2 = 9468 x 10^{-4} $M^{-1}s^{-1}$). *Conditions to generate **2**: 0.5 mM **1** in 3:1 CH_3CN:H_2O + 10 eq. $HClO_4$ and 10 eq. aqueous NaOCl*.

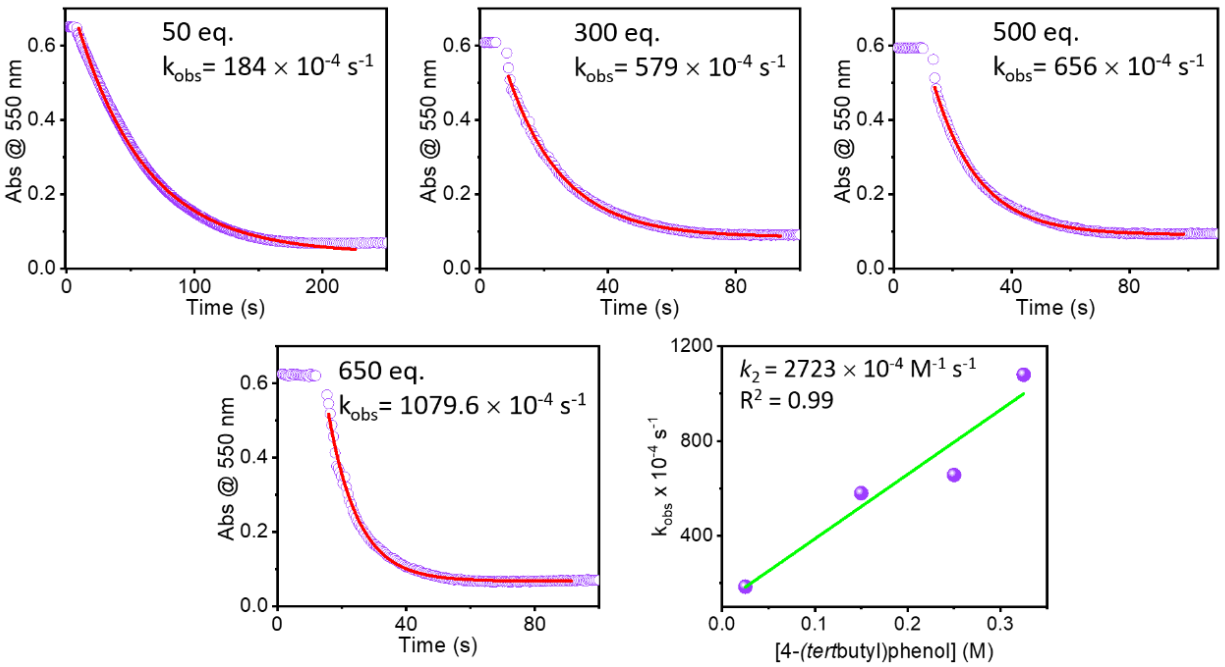

Figure S33: Decay of **2** followed at 550 nm in presence of various concentrations of 4-*tert*butylphenol to give pseudo-first-order rate constants (k_{obs}) in 3:1 CH_3CN: H_2O at 25 °C. The plot of k_{obs} against the concentrations of 4-*tert*butylphenol to obtain a second-order-rate constant (k_2 = 2723 x 10^{-4} $M^{-1}s^{-1}$). *Conditions to generate **2**: 0.5 mM **1** in 3:1 CH_3CN:H_2O + 10 eq. $HClO_4$ and 10 eq. aqueous NaOCl.*

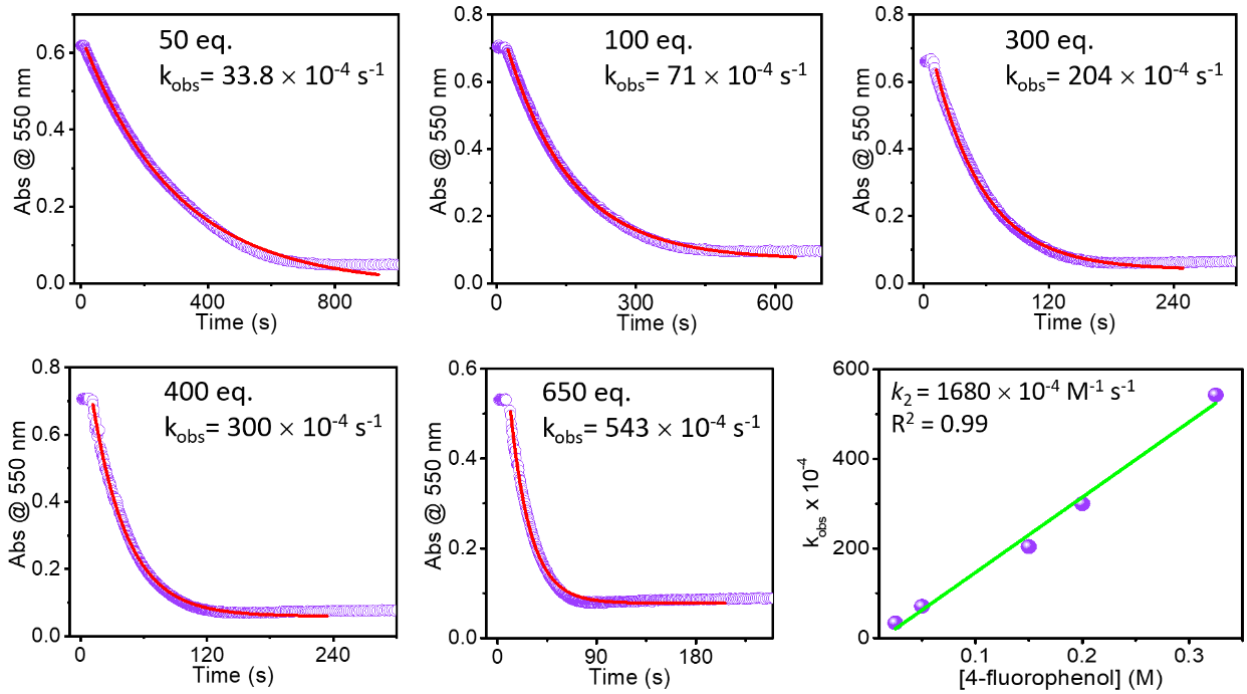

Figure S34: Decay of **2** followed at 550 nm in presence of various concentrations of 4-fluorophenol to give pseudo-first-order rate constants (k_{obs}) in 3:1 CH_3CN: H_2O at 25 °C. The plot of k_{obs} against the concentrations of 4-fluorophenol to obtain a second-order-rate constant (k_2 = 1680 x 10^{-4} $M^{-1}s^{-1}$). *Conditions to generate **2**: 0.5 mM **1** in 3:1 CH_3CN:H_2O + 10 eq. $HClO_4$ and 10 eq. aqueous NaOCl.*

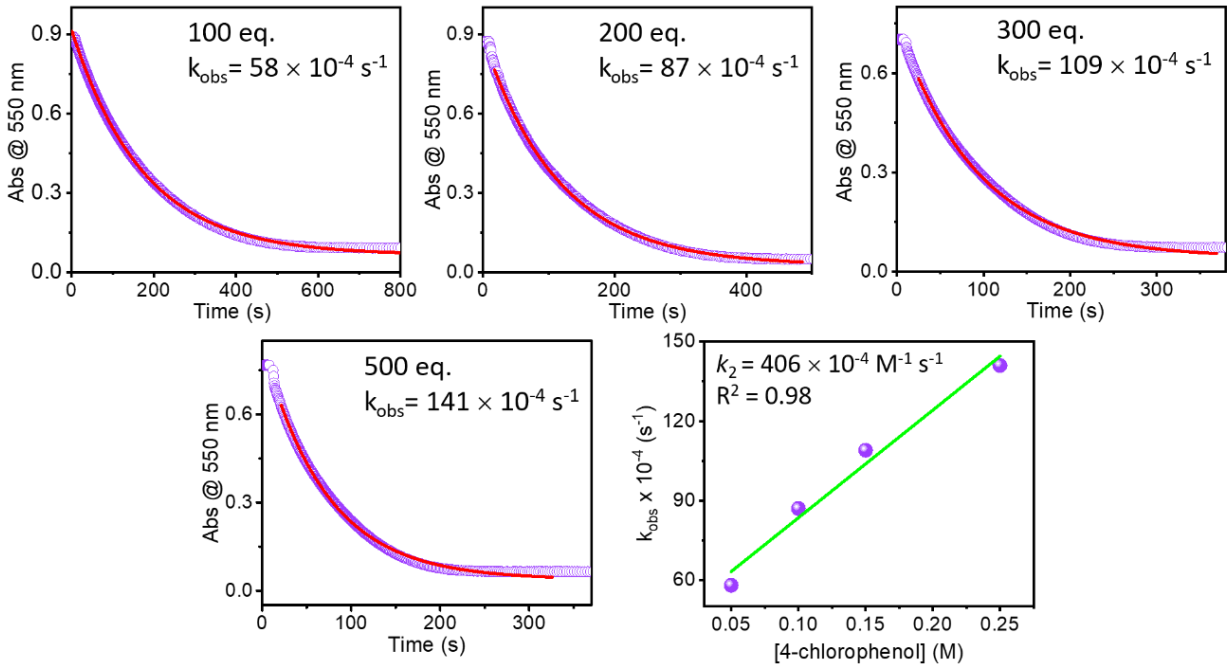

Figure S35: Decay of **2** followed at 550 nm in presence of various concentrations of 4-chlorophenol to give pseudo-first-order rate constants (k_{obs}) in 3:1 CH_3CN: H_2O at 25 °C. The plot of k_{obs} against the concentrations of 4-chlorophenol to obtain a second-order-rate constant (k_2 = 406 x 10^{-4} $M^{-1}s^{-1}$). *Conditions to generate **2**: 0.5 mM **1** in 3:1 CH_3CN:H_2O + 10 eq. $HClO_4$ and 10 eq. aqueous NaOCl*.

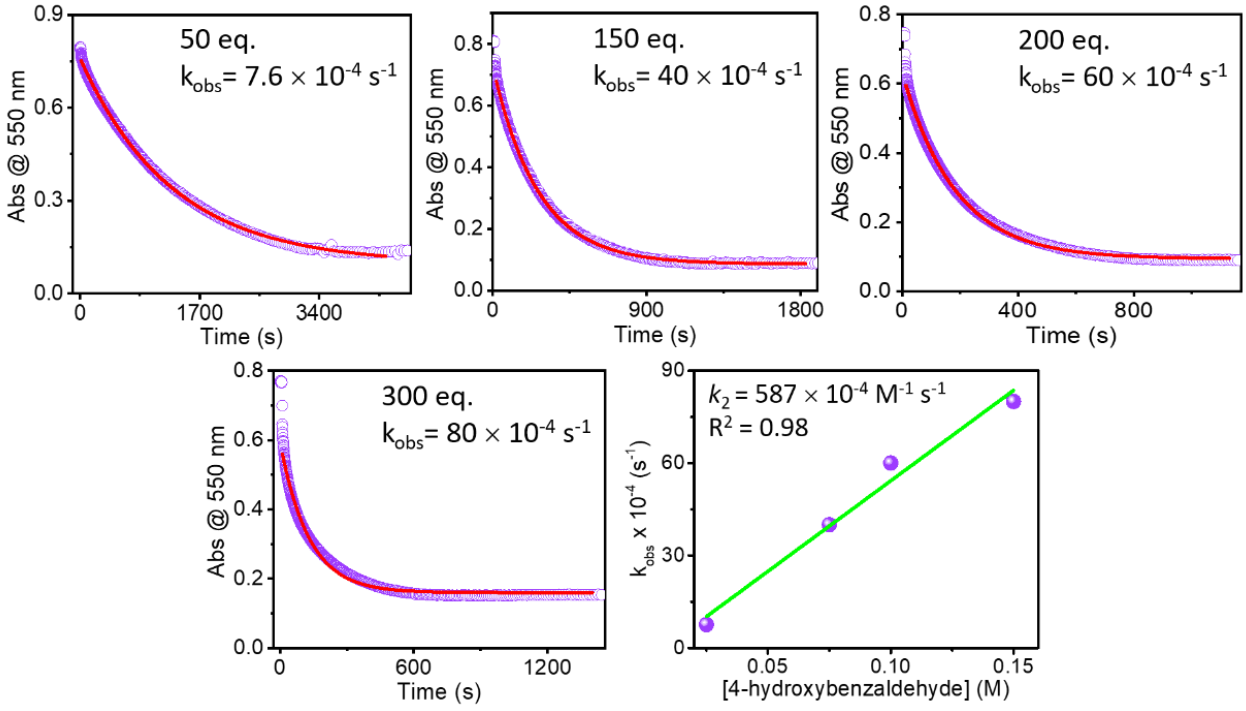

Figure S36: Decay of **2** followed at 550 nm in presence of various concentrations of 4-hydroxybenzaldehyde to give pseudo-first-order rate constants (k_{obs}) in 3:1 CH_3CN: H_2O at 25 °C. The plot of k_{obs} against the concentrations of 4-hydroxybenzaldehyde to obtain a second-order-rate constant (k_2 = 587 x 10^{-4} $M^{-1}s^{-1}$). *Conditions to generate **2**: 0.5 mM **1** in 3:1 CH_3CN:H_2O + 10 eq. $HClO_4$ and 10 eq. aqueous NaOCl*.

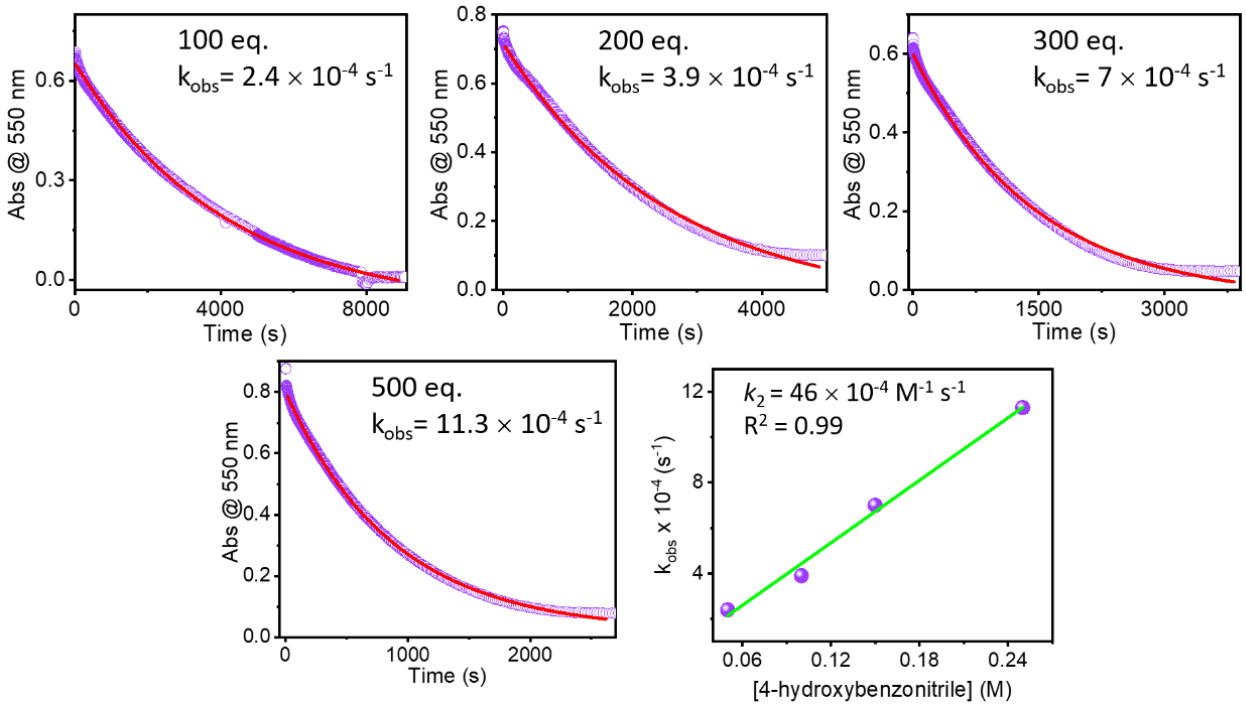

Figure S37: Decay of **2** followed at 550 nm in presence of various concentrations of 4-hydroxybenzonitrile to give pseudo-first-order rate constants (k_{obs}) in 3:1 CH_3CN: H_2O at 25 °C. The plot of k_{obs} against the concentrations of 4-hydroxybenzonitrile to obtain a second-order-rate constant (k_2 = 46 x 10^{-4} M^{-1}s^{-1}). *Conditions to generate **2**: 0.5 mM **1** in 3:1 CH_3CN:H_2O + 10 eq. $HClO_4$ and 10 eq. aqueous NaOCl*.

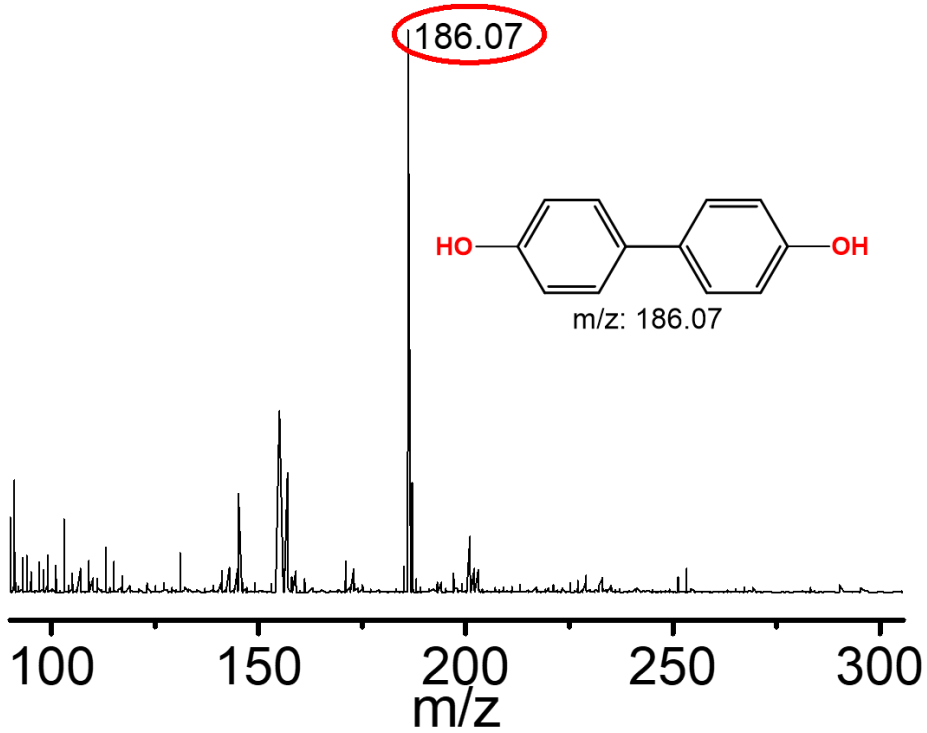

Figure S38: Product analysis of the reaction of **2** with 10 eq. phenol by APCI-MS. Conditions to generate **2**: 2.0 mM **1** in 3:1 CH_3CN:H_2O + 10 eq. $HClO_4$ and 10 eq. aqueous NaOCl.

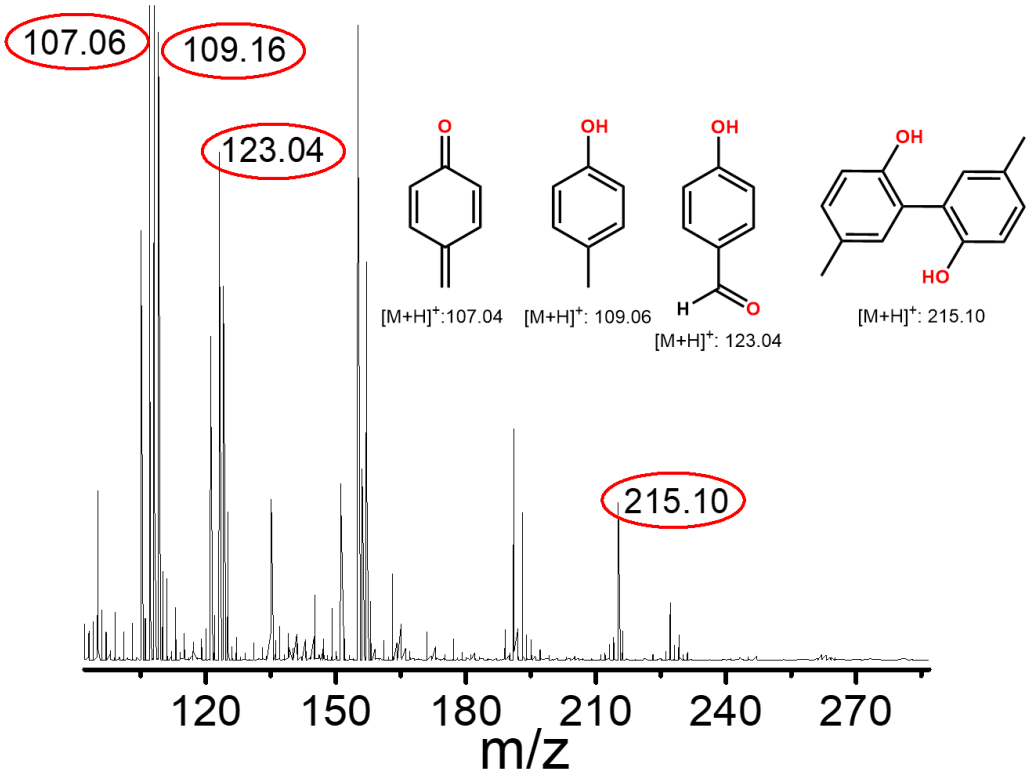

Figure S39: Product analysis of the reaction of **2** with 10 eq. *p*-cresol by APCI-MS. Conditions to generate **2**: 2.0 mM **1** in 3:1 CH_3CN:H_2O + 10 eq. $HClO_4$ and 10 eq. aqueous NaOCl.

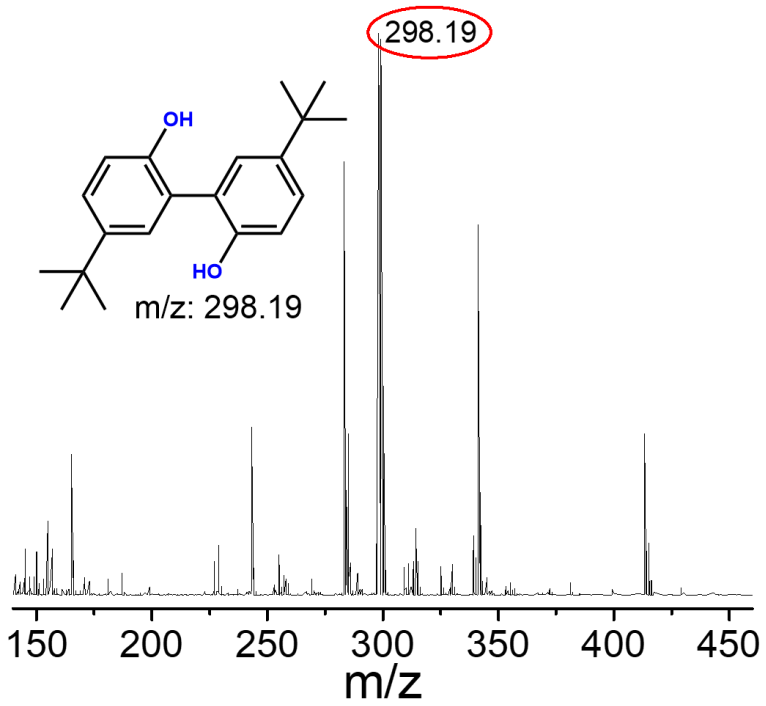

Figure S40: Product analysis of the reaction of **2** with 10 eq. 4-(*tert*-butyl)phenol by APCI-MS. Conditions to generate **2**: 2.0 mM **1** in 3:1 CH_3CN:H_2O + 10 eq. $HClO_4$ and 10 eq. aqueous NaOCl.

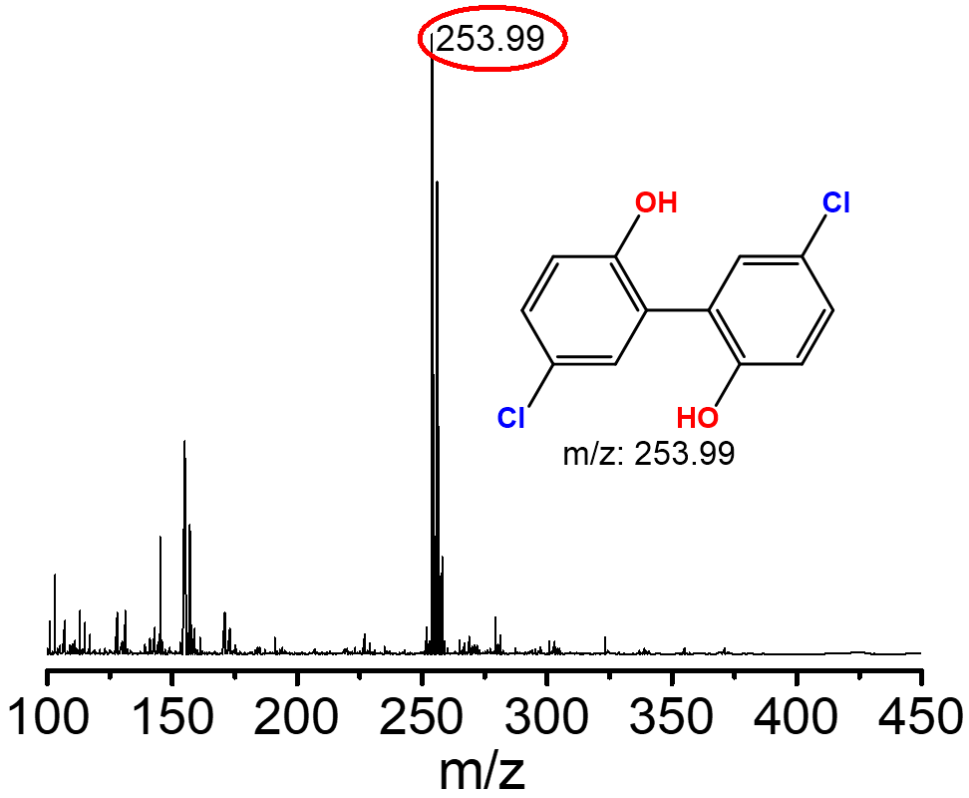

Figure S41: Product analysis of the reaction of **2** with 10 eq. 4-fluorophenol by APCI-MS. Conditions to generate **2**: 2.0 mM **1** in 3:1 CH_3CN:H_2O + 10 eq. $HClO_4$ and 10 eq. aqueous NaOCl.

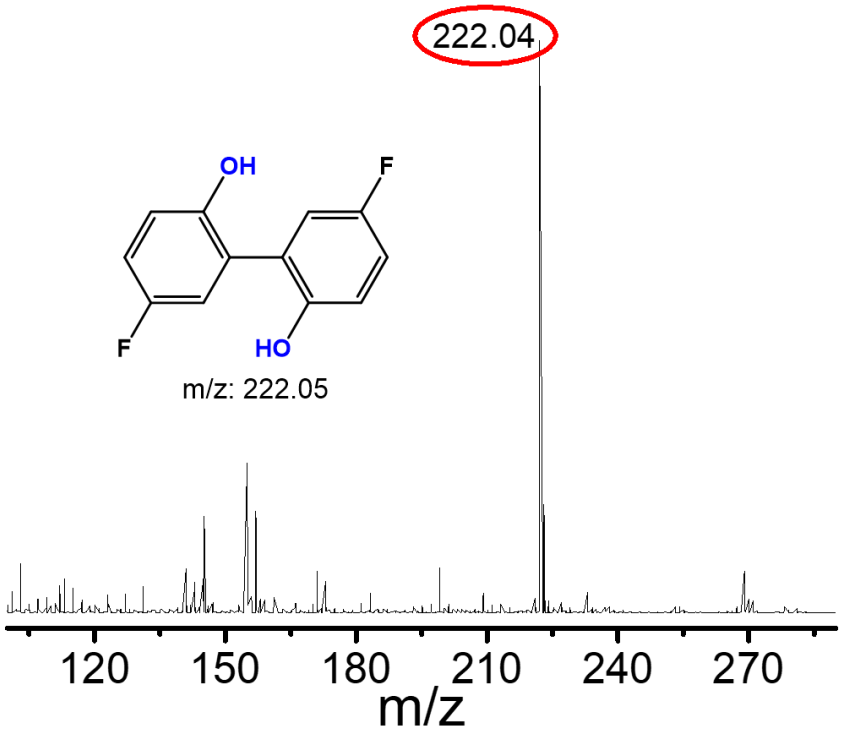

Figure S42: Product analysis of the reaction of **2** with 10 eq. 4-chlorophenol by APCI-MS. Conditions to generate **2**: 2.0 mM **1** in 3:1 CH_3CN:H_2O + 10 eq. $HClO_4$ and 10 eq. aqueous NaOCl.

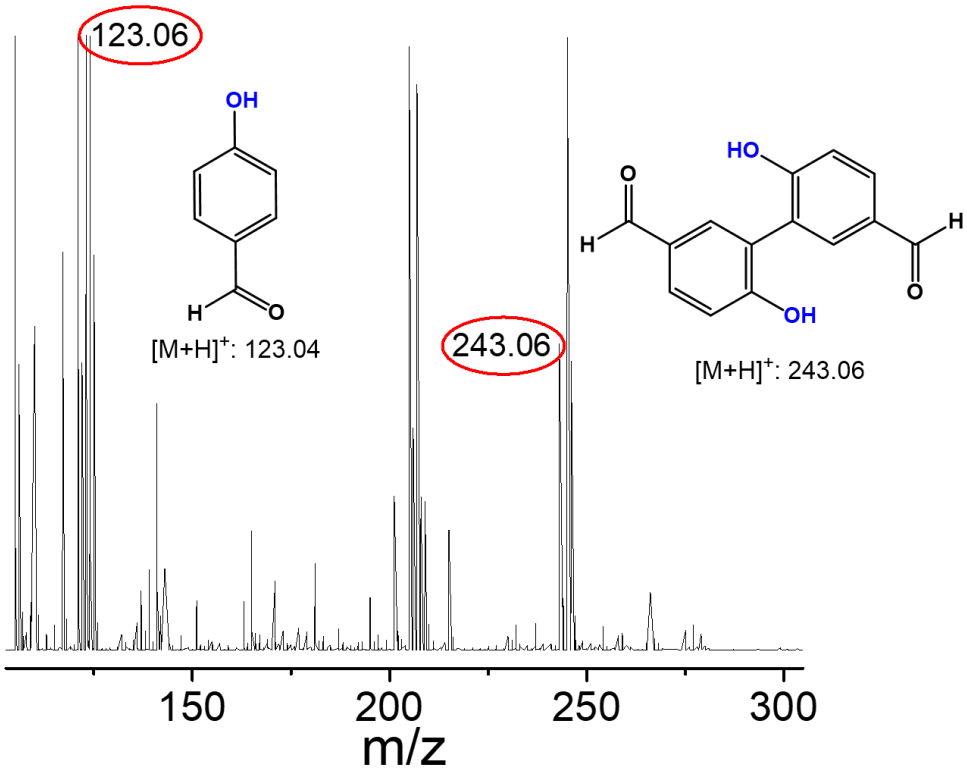

Figure S43: Product analysis of the reaction of **2** with 10 eq. 4-hydroxybenzaldehyde by APCI-MS. Conditions to generate **2**: 2.0 mM **1** in 3:1 CH_3CN:H_2O + 10 eq. $HClO_4$ and 10 eq. aqueous NaOCl.

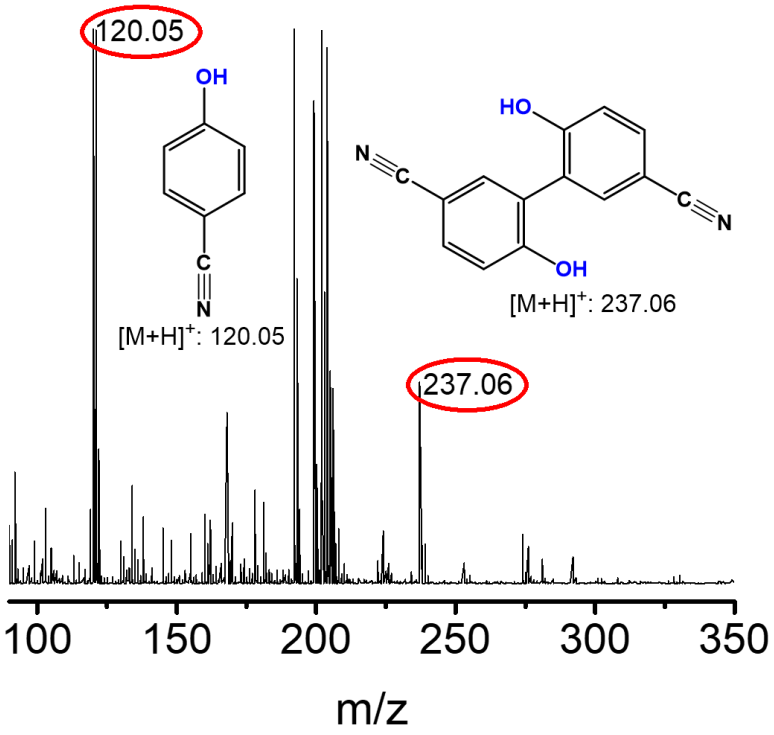

Figure S44: Product analysis of the reaction of **2** with 10 eq. 4-hydroxybenzonitrile by APCI-MS. Conditions to generate **2**: 2.0 mM **1** in 3:1 CH_3CN:H_2O + 10 eq. $HClO_4$ and 10 eq. aqueous NaOCl.

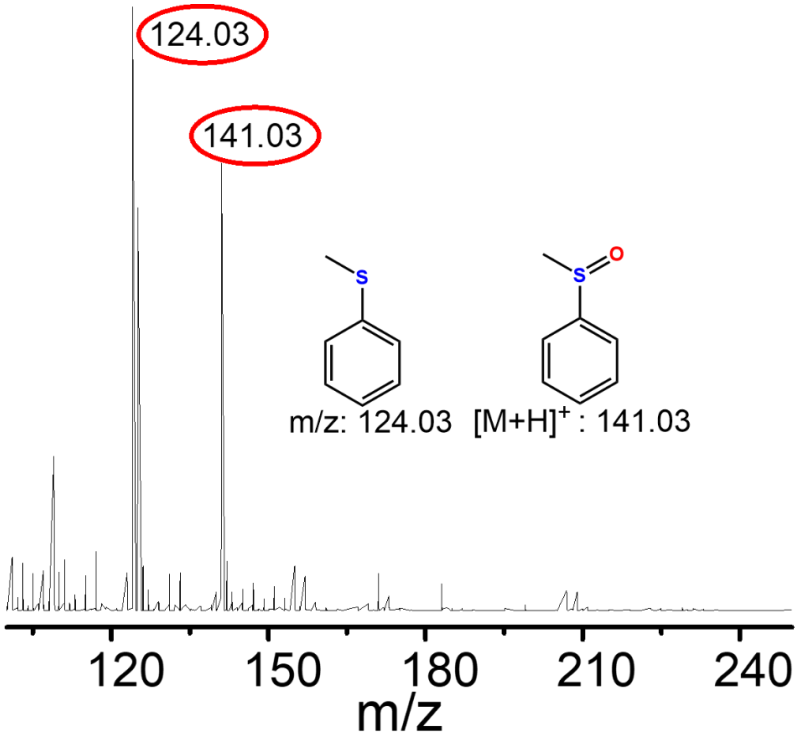

Figure S45: Product analysis of the reaction of thioanisole by APCI-MS. Reaction Conditions: 10 eq. thioanisole (8.5 M, 19 µL in 3:1 CH_3CN:H_2O (1500 µL + 500 µL) + 1 eq. $HClO_4$ (2 M, 8.32 µL) + 10 eq. aqueous NaOCl (2 M, 8.32 µL).

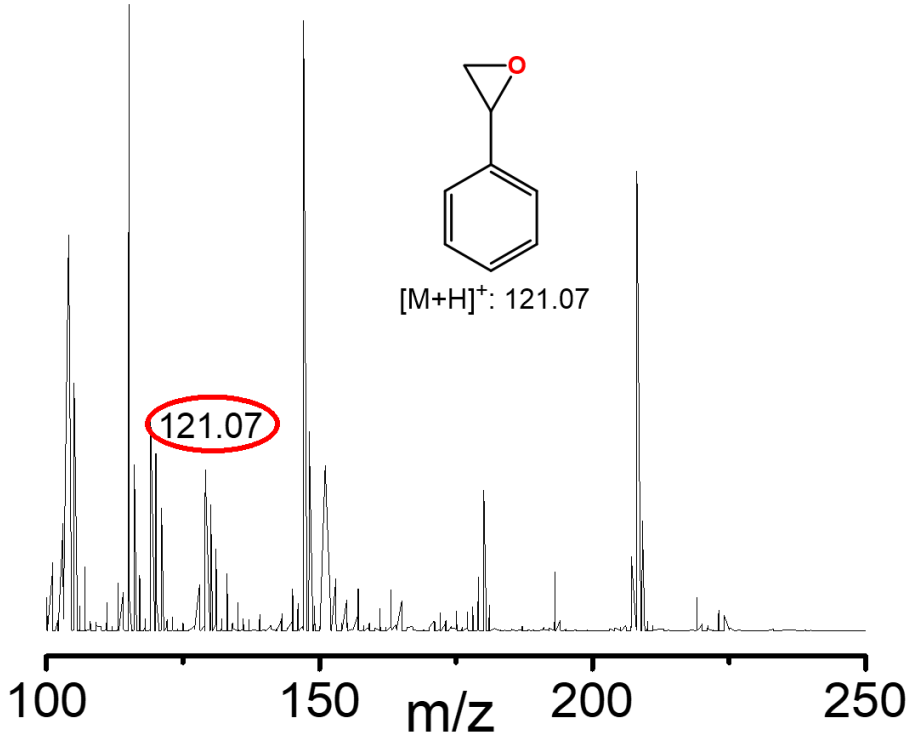

Figure S46: Product analysis of the reaction of styrene by APCI-MS. Reaction Conditions: 10 eq. Styrene (8.7 M, 22 µL) in 3:1 CH_3CN:H_2O (1500 µL + 500 µL) + 1 eq. $HClO_4$ (2 M, 10 µL) + 10 eq. aqueous NaOCl (2 M, 10 µL).

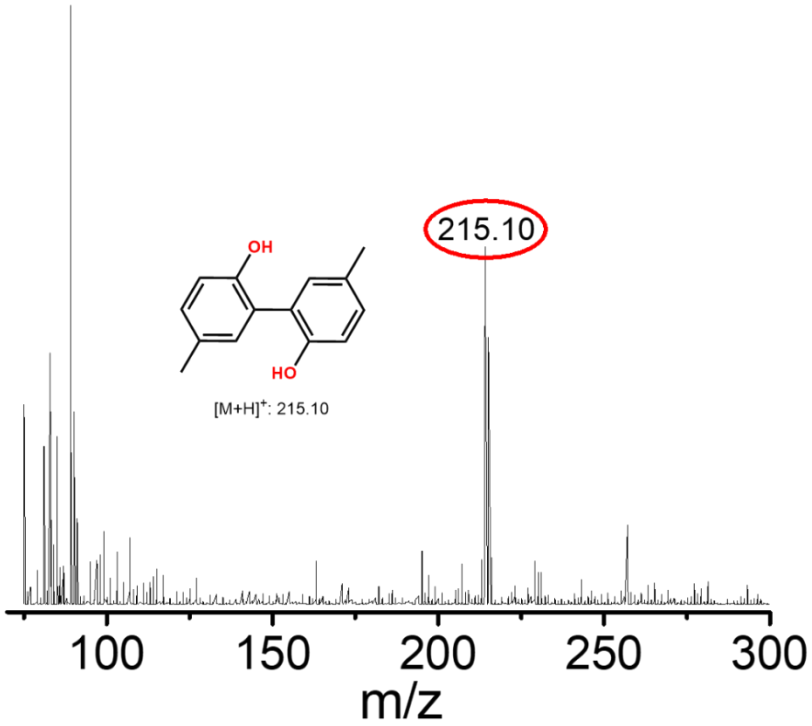

Figure S47: Product analysis of the reaction of *p*-cresol by APCI-MS. Reaction Conditions: 1 eq. *p*-cresol (4.3 mg) in 3:1 CH_3CN:H_2O (1500 µL + 500 µL) + 1 eq. $HClO_4$ (2 M, 20 µL) + 1 eq. aqueous NaOCl (2 M, 20 µL).

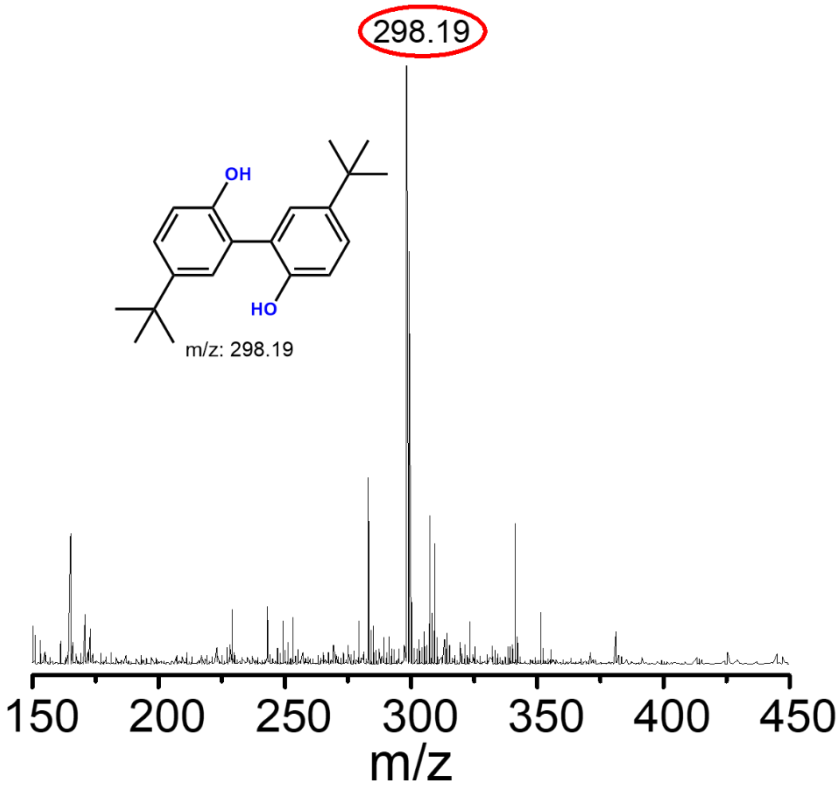

Figure S48: Product analysis of the reaction of 4-(*tert*-butyl)phenol by APCI-MS. Reaction Conditions: 1 eq. 4-(*tert*-butyl)phenol (6 mg) in 3:1 CH_3CN:H_2O (1500 µL + 500 µL) + 1 eq. $HClO_4$ (2 M, 20 µL) + 1 eq. aqueous NaOCl (2 M, 20 µL).

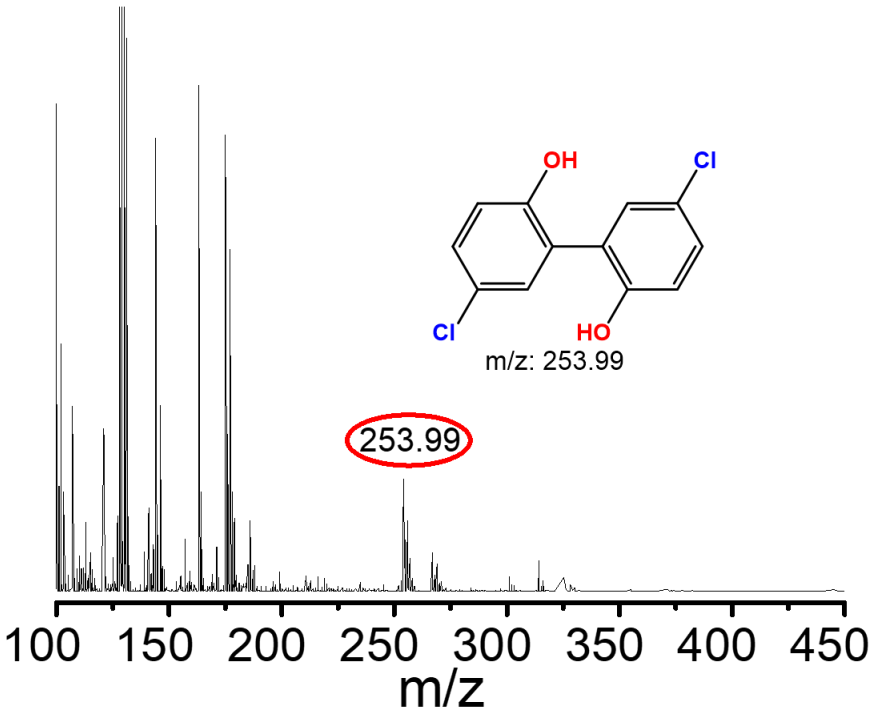

Figure S49: Product analysis of the reaction of 4-chlorophenol by APCI-MS. Reaction Conditions: 1 eq. 4-chlorophenol (5.1 mg) in 3:1 CH_3CN:H_2O (1500 µL + 500 µL) + 1 eq. $HClO_4$ (2 M, 20 µL) + 1 eq. aqueous NaOCl (2 M, 20 µL).

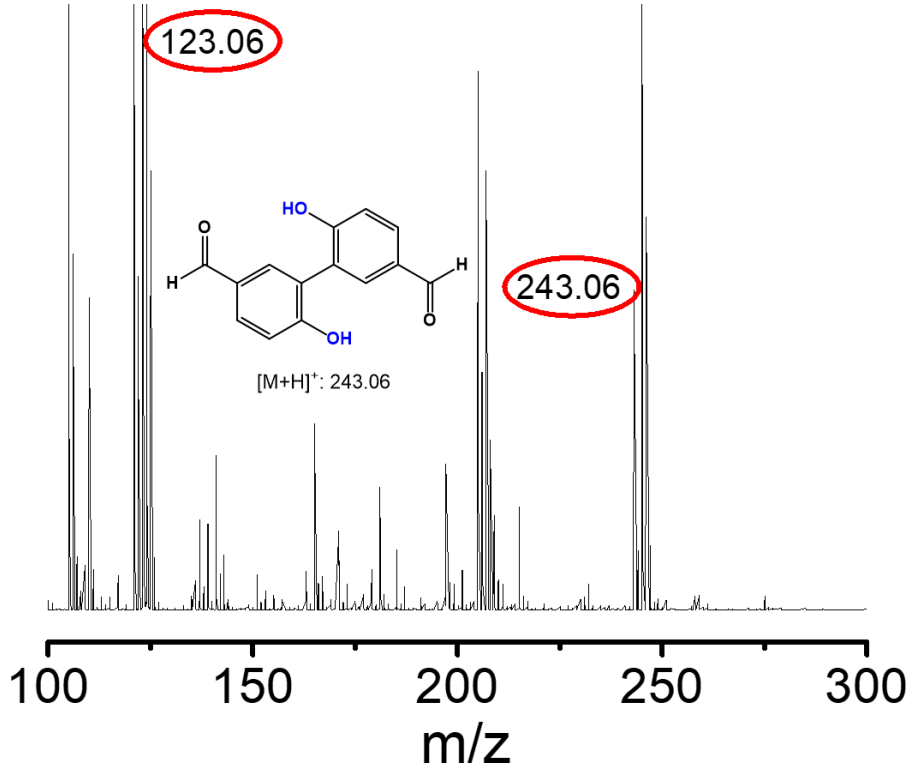

Figure S50: Product analysis of the reaction of 4-hydroxybenzaldehyde by APCI-MS. Reaction Conditions: 1 eq. 4-hydroxybenzaldehyde (4.88 mg) in 3:1 CH_3CN:H_2O (1500 µL + 500 µL) + 1 eq. $HClO_4$ (2 M, 20 µL) + 1 eq. aqueous NaOCl (2 M, 20 µL).

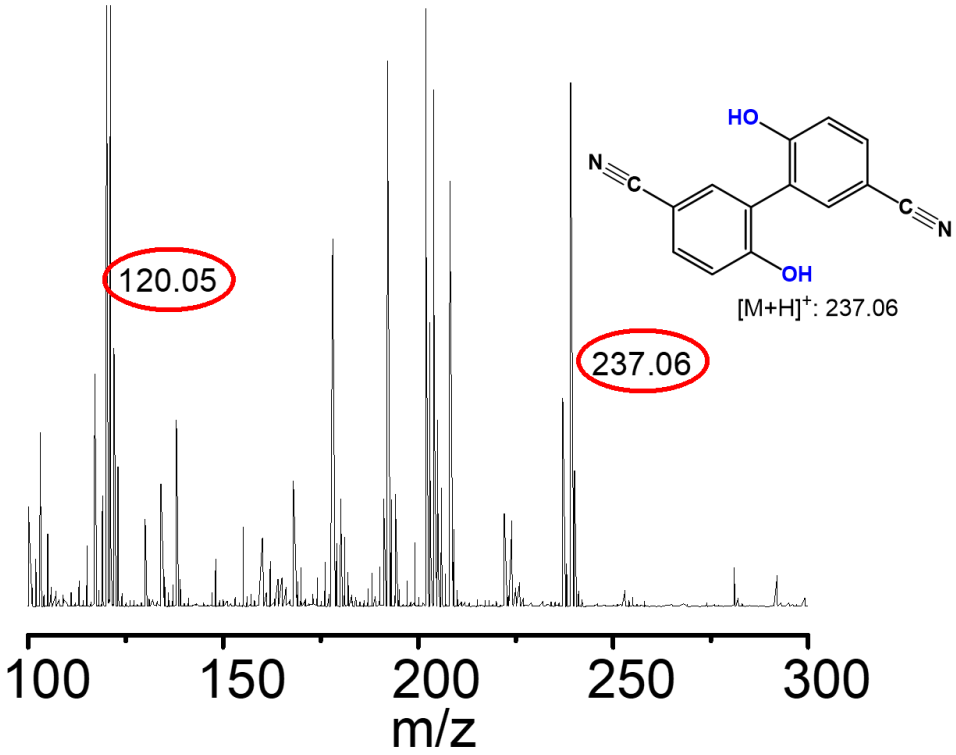

Figure S51: Product analysis of the reaction of 4-hydroxybenzonitrile by APCI-MS. Reaction Conditions: 1 eq. 4-hydroxybenzonitrile (4.76 mg) in 3:1 CH_3CN:H_2O (1500 µL + 500 µL) + 1 eq. $HClO_4$ (2 M, 20 µL) + 1 eq. aqueous NaOCl (2 M, 20 µL).

References:

[1] L. Duelund, R. Hazell, C. J. McKenzie, L. P. Nielsen and H. Toftlund, *J. Chem. Soc. Dalton Trans*., 2001, **2**, 152–156.

[2] R. Sharma, J. D. Knoll, P. D. Martin, I. Podgorski, C. Turro and J. J. Kodanko, *Inorg. Chem.,* 2014, **53**, 3272−3274.

[3] S. Ohzu, T. Ishizuka, Y. Hirai, H. Jiang, M. Sakaguchi, T. Ogura, S. Fukuzumi and T. Kojima, *Chem. Sci.,* 2012, **3**, 3421-3431.